

ANSI/ASA S1.18-2010
(Revision of ANSI S1.18-1999)

AMERICAN NATIONAL STANDARD

Method for Determining the Acoustic Impedance of Ground Surfaces

ANSI/ASA S1.18-2010

Accredited Standards Committee S1, Acoustics

Standards Secretariat
Acoustical Society of America
35 Pinelawn Road, Suite 114 E
Melville, NY 11747-3177

The American National Standards Institute, Inc. (ANSI) is the national coordinator of voluntary standards development and the clearinghouse in the U.S.A. for information on national and international standards.

The Acoustical Society of America (ASA) is an organization of scientists and engineers formed in 1929 to increase and diffuse the knowledge of acoustics and to promote its practical applications.



AMERICAN NATIONAL STANDARD

**Method for Determining the Acoustic Impedance of
Ground Surfaces**

Secretariat:

Acoustical Society of America

Approved May 28, 2010 by:

American National Standards Institute, Inc.

Abstract

This Standard describes procedures for obtaining the real and imaginary parts of normalized acoustic impedance ratio of ground surfaces from *in-situ* measurements of the sound pressure levels at two vertically separated microphones using specified geometries and the averaged values of the difference between the simultaneous instantaneous sound-pressure signals at the two microphones. It extends and revises the template method given in the 1999 edition to enable the user to obtain values of the normalized specific acoustic impedance ratio of the ground entirely from measurements and independently of any model for the acoustic impedance of the ground surface except as a check on the validity of the resulting values.

AMERICAN NATIONAL STANDARDS ON ACOUSTICS

The Acoustical Society of America (ASA) provides the Secretariat for Accredited Standards Committees S1 on Acoustics, S2 on Mechanical Vibration and Shock, S3 on Bioacoustics, S3/SC 1 on Animal Bioacoustics, and S12 on Noise. These committees have wide representation from the technical community (manufacturers, consumers, trade associations, organizations with a general interest, and government representatives). The standards are published by the Acoustical Society of America as American National Standards after approval by their respective Standards Committees and the American National Standards Institute (ANSI).

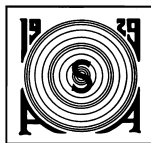
These standards are developed and published as a public service to provide standards useful to the public, industry, and consumers, and to Federal, State, and local governments.

Each of the Accredited Standards Committees (operating in accordance with procedures approved by ANSI) is responsible for developing, voting upon, and maintaining or revising its own Standards. The ASA Standards Secretariat administers Committee organization and activity and provides liaison between the Accredited Standards Committees and ANSI. After the Standards have been produced and adopted by the Accredited Standards Committees, and approved as American National Standards by ANSI, the ASA Standards Secretariat arranges for their publication and distribution.

An American National Standard implies a consensus of those substantially concerned with its scope and provisions. Consensus is established when, in the judgment of the ANSI Board of Standards Review, substantial agreement has been reached by directly and materially affected interests. Substantial agreement means much more than a simple majority, but not necessarily unanimity. Consensus requires that all views and objections be considered and that a concerted effort be made towards their resolution.

The use of an American National Standard is completely voluntary. Their existence does not in any respect preclude anyone, whether he or she has approved the Standards or not, from manufacturing, marketing, purchasing, or using products, processes, or procedures not conforming to the Standards.

NOTICE: This American National Standard may be revised or withdrawn at any time. The procedures of the American National Standards Institute require that action be taken periodically to reaffirm, revise, or withdraw this Standard.



Acoustical Society of America
ASA Secretariat
35 Pinelawn Road, Suite 114E
Melville, New York 11747-3177
Telephone: 1 (631) 390-0215
Fax: 1 (631) 390-0217
E-mail: asastds@aip.org

© 2010 by Acoustical Society of America. This Standard may not be reproduced in whole or in part in any form for sale, promotion, or any commercial purpose, or any purpose not falling within the provisions of the U.S. Copyright Act of 1976, without prior written permission of the publisher. For permission, address a request to the Standards Secretariat of the Acoustical Society of America.

Contents

1	Scope	1
2	Normative references	1
3	Terms and definitions	2
4	Measurement method.....	2
4.1	Recommended geometries	2
4.2	Time convention	3
4.3	Measurement procedure	4
4.4	Ground and environmental conditions	4
4.5	Determination of the normalized specific acoustic impedance ratio	5
4.6	Procedure to determine best fit in Step 1	7
4.7	Minimization procedure for Step 2	8
5	Required instruments for measuring ground impedance outdoors	9
5.1	Sound source	9
5.2	Microphones	10
5.3	Calibration	10
5.4	Sound level meter/analyzer.....	10
5.5	Miscellaneous.....	11
5.6	Configuration of measuring system.....	11
5.7	Wind speed	11
6	Measurement.....	11
6.1	Area of ground.....	11
6.2	Data collection.....	11
7	Data reduction	12
7.1	Corrections	12
7.2	Experimental error.....	12
8	Reporting	13
8.1	Introductory information	13
8.2	Documentation of the instrumentation	13
8.3	Meteorological data	13
8.4	Impedance values	13
8.5	Other observations.....	13
9	Templates for obtaining normalized surface impedance model parameters	14
9.1	Templates for the one-parameter impedance model.....	14
9.2	Templates for the two-parameter normalized surface impedance model.....	16
Annex A	(informative) Worked examples of procedure.....	22
A.1	Example 1: Cricket field at the Open University, UK.....	22
A.2	Example 2: Institutional grass at the National Research Council, Canada	27
A.3	Example 3: University lawn in Germany	33

A.4 Example 4: Granite gravel road on U.S. Army Research Laboratory testing facility.....	37
Annex B (informative) Example impedance parameters	40
B.1 One-parameter model	40
B.2 Two-parameter model	40
Annex C (informative) Formulae for the complex sound pressure ratio	41
Annex D (informative) Mathematical functions	43
Annex E (informative) Software for deduction of surface impedance according to ANSI/ASA S1.18-2010.....	46
Bibliography	47

Tables

Table 1 – Template 1A—Pre-calculated level differences (dB) for geometry A using the one- parameter model.....	14
Table 2 – Template 1B—Pre-calculated level differences (dB) for geometry B using the one- parameter model.....	15
Table 3 – Template 2A—Pre-calculated level differences (dB) for geometry A using the two- parameter model.....	16
Table 4 – Template 2B—Pre-calculated level differences (dB) for geometry B using the two- parameter model.....	19
Table A.1 – Cumulative error, E , for the one-parameter templates, computed using Equation (8) in 4.6	23
Table A.2 – Cumulative error, E , for the two-parameter templates, computed using Equation (8) in 4.6	25
Table A.3 – Cumulative error, E , for the one-parameter templates, computed using Equation (8) in 4.6	28
Table A.4 – Cumulative error, E , for the two-parameter templates, computed using Equation (8) in 4.6	28
Table A.5 – Cumulative error, E , for Example 2	34
Table B.1 – Parameter values obtained using one-parameter model	40
Table B.2 – Parameter values obtained using two-parameter model.....	40

Figures

Figure 1 – Geometrical definitions: h_s = source height, h_t = top microphone height, h_b = bottom microphone height, d = source/receiver horizontal separation	3
Figure 2 – Point source and vertically separated microphones at the Open University, UK.....	10
Figure 3b – Template curves for geometry B and eight values of effective flow resistivity, σ_{eff} , between 10 and 3200 kPa s/m ²	15
Figure 4a – Template curves for geometry A with $\alpha_e = 3/\text{m}$ and four values of effective flow resistivity, σ_e (10, 32, 100, and 1000 kPa s/m ²)	17
Figure 4b – Template curves for geometry A with $\alpha_e = 50/\text{m}$ and three values of effective flow resistivity	17
Figure 4c – Template curves for geometry A with $\alpha_e = 100/\text{m}$ and three values of effective flow resistivity, σ_e (10, 100, and 1000 kPa s/m ²)	18
Figure 4d – Template curves for geometry A with $\alpha_e = 250/\text{m}$ and three values of effective flow resistivity, σ_e (10, 100, and 1000 kPa s/m ²)	18
Figure 5a – Template curves for geometry B with $\alpha_e = 3/\text{m}$ and four values of effective flow resistivity, σ_e (10, 32, 100, and 1000 kPa s/m ²)	20
Figure 5b – Template curves for geometry B with $\alpha_e = 50/\text{m}$ and three values of effective flow resistivity	20
Figure 5c – Template curves for geometry B with $\alpha_e = 100/\text{m}$ and three values of effective flow resistivity, σ_e (10, 100, and 1000 kPa s/m ²)	21
Figure 5d – Template curves for geometry B with $\alpha_e = 250/\text{m}$ and three values of effective flow resistivity, σ_e (10, 100, and 1000 kPa s/m ²)	21
Figure A.1 – Template plots for one-parameter impedance model	22
Figure A.2 – Comparisons of measured LD spectra with two-parameter model templates	23
Figure A.3 – Normalized specific acoustic impedance ratio deduced from six sets of averaged complex sound pressure ratios. Those deduced from geometry B are plotted as broken lines. The mean values are plotted as dotted lines.	25
Figure A.4 – A comparison of normalized specific acoustic impedance ratio spectra deduced from Steps 1 and 2 (broken line)	26
Figure A.5 – Template method (Step 1) using data obtained with a single microphone.....	27

Figure A.6 – Template for geometry A and the one-parameter model with superimposed NRC data	27
Figure A.7 – Template for geometry B and the one-parameter model with superimposed NRC data	28
Figure A.8(a) – Template for geometry A and the two-parameter model with superimposed NRC data	29
Figure A.8(b) – Template for geometry A and the two-parameter model with superimposed NRC data	29
Figure A.9(a) – Template for geometry B and the two-parameter model with superimposed NRC data	30
Figure A.9(b) – Template for geometry B and the two-parameter model with superimposed NRC data	30
Figure A.10 – Normalized specific acoustic impedance ratio deduced from the measured complex sound pressure ratios using geometry A.....	31
Figure A.11 – Normalized surface impedance spectra deduced from Step 1 (one-parameter model – solid line, two parameter model – dash and dotted line) and Step 2 (thicker continuous lines)	32
Figure A.12 – Normalized surface impedance spectra deduced from Step 1 (one-parameter model – solid line, two parameter model – dashed lines and dotted line) and Step 2 (thicker continuous lines)	32
Figure A.13 – Data and one-parameter model templates for geometries A and B.....	33
Figure A.14 – Data and 2-parameter model templates for geometries A and B.....	34
Figure A.15 – Deduced normalized surface impedance ratio spectra using all ten measurements	35
Figure A.16 – Smoothed normalized specific acoustic impedance ratio deduced using geometry B.....	36
Figure A.17 – Normalized specific acoustic impedance ratio spectra deduced from both geometries A and B and best-fit impedance model predictions	36
Figure A.18 – ARL data superimposed on one-parameter templates (a) geometry A and (b) geometry B.....	37
Figure A.19 (a) to (h) – ARL Gravel road data superimposed on two-parameter templates.....	38
Figure A.19 a to h (continued) – ARL Gravel road data superimposed on two-parameter templates	39

Foreword

[This Foreword is for information only and is not a part of the American National Standard ANSI/ASA S1.18-2010 American National Standard Method for Determining the Acoustic Impedance of Ground Surfaces.]

This Standard comprises a part of a group of definitions, standards, and specifications for use in acoustics. It was developed and approved by Accredited Standards Committee S1, Acoustics, under its approved operating procedures. Those procedures have been accredited by the American National Standards Institute (ANSI). The Scope of Accredited Standards Committee S1 is as follows:

Standards, specifications, methods of measurement and test, and terminology in the field of physical acoustics, including architectural acoustics, electroacoustics, sonics and ultrasonics, and underwater sound, but excluding those aspects which pertain to biological safety, tolerances, and comfort.

This Standard is a revision of ANSI S1.18-1999, which has been technically revised. The template method is augmented by a procedure to utilize measurements of the magnitude and relative phase of the averaged ratio of the difference between instantaneous sound-pressure signals at two specific locations relative to the location of a sound source and thereby deduce the real and imaginary parts of the complex normalized specific acoustic impedance ratio.

This Standard is not comparable to any existing ISO Standard.

This Standard includes 5 Annexes, all of which are informative and are not considered part of this Standard.

The software provided with this American National Standard is entirely informative and provided for the convenience of the user. Use of the provided software is not required for conformance with the Standard.

ASA and the owners of the copyright to the software provided with this American National Standard make no other representation or warranty or condition of any kind, whether express or implied (either in fact or by operation of law) with respect to any part of the product, including, without limitation, with respect to the sufficiency, accuracy or utilization of, or any information or opinion contained or reflected in, any of the product. ASA and the owners expressly disclaim all warranties or conditions of merchantability or fitness for a particular purpose. No officer, director, employee, member, agent, representative, or publisher of the copyright holder is authorized to make any modification, extension, or addition to this limited warranty.

At the time this Standard was submitted to Accredited Standards Committee S1, Acoustics, for approval, the membership was as follows:

- P. Battenberg, *Chair*
- R.J. Peppin, *Vice-Chair*
- S.B. Blaeser, *Secretary*

Acoustical Society of America A.H. Marsh
..... P.D. Schomer (Alt.)

Air-Conditioning, Heating and Refrigeration Institute	S. Lind
	D. Brown (Alt.)
American Academy of Audiology	D. Ostergren
American Industrial Hygiene Association	D. Driscoll
	D. Sandfort (Alt.)
Bruel & Kjaer Instrumentation, Inc.	M. Alexander
	J. Chou (Alt.)
Campanella Associates	A.J. Campanella
ETS-Lindgren Acoustic Systems	D. Winker
	M. Black (Alt.)
G.R.A.S. Sound & Vibration	B. Schustrich
Information Technology Industry Council	M.A. Nobile
	J. Rosenberg (Alt.)
National Council of Acoustical Consultants	G.E. Winzer
	E. Logsdon (Alt.)
National Institute of Standards & Technology (NIST)	V. Nedzelitsky
	D.J. Evans (Alt.)
PCB Group	K. Cox
	L. Harbaugh (Alt.)
Quest Technologies, Inc.	P. Battenberg
	M. Wurm (Alt.)
Scantek, Inc.	R.J. Peppin
	M. Buzduga (Alt.)
U.S. Air Force (USAF)	R. McKinley
	F. Mobey (Alt.)
U.S. Army Construction Engineering Research Laboratory	M. Swearingen
	M.J. White (Alt.)
U.S. Army Research Laboratory, Human Research and Engineering Directorate	T.R. Letowski
	A. Scharine (Alt.)

Individual Experts of Accredited Standards Committee S1, Acoustics, were:

S.L. Ehrlich
K.M. Eldred
W.J. Galloway

W.W. Lang
A.H. Marsh
P.D. Schomer

J.P. Seiler
G.S.K. Wong
L. Wu

Working Group S1/WG 20, Measurement of Ground Impedance and Attenuation of Sound due to the Ground, which assisted Accredited Standards Committee S1, Acoustics, in the development of this Standard, had the following membership.

K. Attenborough, Chair
J.M. Sabatier, Vice-Chair

W.C.K. Alberts, II
G.A. Daigle
R. Kruse

K.M. Li
V. Mellert
M. Stinson

L.C. Sutherland
S. Taherzadeh
A. Zuckerwar

Suggestions for improvements to this Standard will be welcomed. They should be sent to Accredited Standards Committee S1, Acoustics, in care of the Standards Secretariat of the Acoustical Society of America, 35 Pinelawn Road, Suite 114E, Melville, New York 11747-3177. Telephone: 631-390-0215; FAX: 631-390-0217; E-mail: asastds@aip.org.

Introduction

Experimental techniques to measure impedance include the use of an impedance tube, techniques that measure the sound pressure levels above a surface, and direct measurements of sound pressure and volume velocity.

This Standard does not consider the direct measurement of sound pressure and volume velocity.

The impedance tube is in common use to measure the acoustic impedance of porous materials. It has the advantage of a straightforward theoretical framework that allows direct determination of both the real and imaginary parts of the impedance. However, its application in the field to obtain ground impedance suffers from two major disadvantages. First, it requires an accurate measurement of the distance from the first interference minimum to an ill-defined test surface, and, secondly, it is invasive. This Standard does not recommend the use of an impedance tube for the measurement of the acoustic impedance of a ground surface.

Techniques that use measurements of sound pressure levels above a surface include several variations based on the type of excitation, angle of incidence, number of microphones, and fitting methods. All enjoy the advantage that the measurement is performed on the ground in its natural condition. However, because of the spherical wavefront, the theoretical framework is mathematically intricate. Annexes C and D detail the expressions and special functions used in the calculations in Clause 4.

.

American National Standard

Method for Determining the Acoustic Impedance of Ground Surfaces

1 Scope

Outdoor sound close to the ground is influenced by the acoustical properties of the ground. This Standard describes recommended procedures to characterize, and the instruments to measure quantities that may be used to deduce, the acoustical properties of ground surfaces. Although this Standard is intended primarily for outdoor measurements, indoor measurement of undisturbed portions of a ground surface, such as sod, is within its scope also.

The Standard yields the real and imaginary parts of the normalized specific acoustic impedance ratio of ground surfaces in the frequency range between 250 and 4000 Hz for outdoor sound propagation predictions. The Standard uses measurements of the interference between direct and ground-reflected sound to deduce both normalized specific acoustic impedance ratio and impedance model parameters. The impedance-ratio model parameters of effective flow resistivity and a porosity factor, determined from best fits to the templates of calculated level differences, may be used to estimate the normalized specific acoustic impedance ratio at frequencies outside the specified range.

The basic purpose of this Standard is to establish uniform procedures for obtaining the real and imaginary parts of the normalized specific acoustic impedance ratio of ground surfaces outdoors.

The method is applicable to all nominally flat, commonly occurring surfaces including grassland or snow-covered ground.

The method is not applicable to rough grounds where the variation in height is greater than half of the shortest wavelength of interest. For the specified upper frequency of 4 kHz this limits the variation in height to about 5 cm. See also Clause 4.4.

2 Normative references

The following referenced documents are indispensable for the application of this Standard. For dated references, only the edition cited applies. For undated references, the latest edition of the referenced document (including any amendments) applies.

ANSI S1.1, American National Standard Acoustical Terminology

ANSI/ASA S1.11, American National Standard Specification for Octave-Band and Fractional-Octave-Band Analog and Digital Filters

ANSI S1.40, American National Standard Specifications and Verification Procedures for Sound Calibrators

IEC 61672-1, Electroacoustics — Sound level meters — Part 1: Specifications

3 Terms and definitions

For the purposes of this Standard, the terms and definitions given in ANSI S1.1 and the following apply:

3.1

specific acoustic impedance, Z_s

at a point in a sound field, quotient of sound pressure by particle velocity

NOTE 1 Unit, pascal per (meter per second) [Pa/(m/s)].

NOTE 2 The real part of the specific acoustic impedance is specific acoustic resistance; the imaginary part is specific acoustic reactance.

3.2

specific acoustic admittance, β

reciprocal of the specific acoustic impedance

NOTE 1 Unit, (meter per second) per pascal [(m/s)/Pa].

NOTE 2 The real part of specific acoustic admittance is specific acoustic conductance; the imaginary part is specific acoustic susceptance.

3.3

normalized specific acoustic impedance ratio

ratio of specific acoustic impedance of a ground surface to the characteristic impedance of air at specified atmospheric conditions

3.4

complex sound pressure ratio

ratio of magnitudes and relative phase of the pressures measured by two spatially separated microphones subjected to sound emitted by the same point source

NOTE This definition is specific to this Standard and is not within the scope of ANSI S1.1-1999 (R 2004).

4 Measurement method

4.1 Recommended geometries

The measurement of level difference spectra shall be conducted using **both of** the following two geometries (see Figure 1):

Geometry A

Source height (h_s) = 0.325 m

Upper microphone height (h_t) = 0.46 m

Lower microphone height (h_b) = 0.23 m

Horizontal separation (d) = 1.75 m

Geometry B

Source height (h_s) = 0.20 m

Upper microphone height (h_t) = 0.20 m

Lower microphone height (h_b) = 0.05 m

Horizontal separation (d) = 1.0 m

Note that these geometries will not yield satisfactory results if the ground impedance is high. But, in this case, accurate values for ground impedance should not be necessary and it is recommended that Steps 2 to 4 be omitted from the procedure detailed in 4.5.1.

Geometry A covers the broadest range of frequencies. Geometry B emphasizes ground effect at frequencies above 1000 Hz and may be better suited for hard grounds.

As long as the horizontal separation of the source and the receiver is not greater than 3.0 m or not less than 1.0 m and the angles of incidence are broadly the same as those for geometries A and B, the user has discretion in the choice of the geometry. However, it is essential that the source and receiver positions be measured as accurately as possible (i.e., to within ± 0.01 m), and the test report shall include information on the geometry used for measurements. If Figures 3a through 4d are used, then the geometry must correspond to those specified above to within ± 0.01 m.

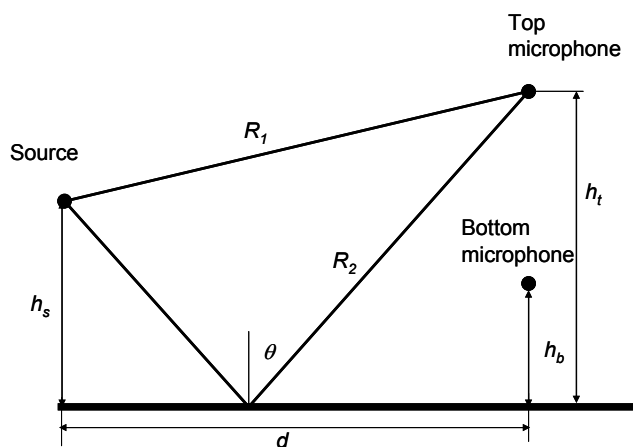


Figure 1 – Geometrical definitions: h_s = source height, h_t = top microphone height, h_b = bottom microphone height, d = source/receiver horizontal separation

4.2 Time convention

A harmonic time dependence of $e^{-i\omega t}$ is assumed throughout this Standard. However, certain spectrum analyzers assume an alternative harmonic time convention of $e^{+i\omega t}$. The user shall ascertain the time dependence used by the analysis equipment. If the alternative dependence is used, the complex sound pressure ratio, $T(f)$, as measured and recorded by such equipment, shall be converted to its conjugate before carrying out the procedure set out in this clause.

4.3 Measurement procedure

The test signal shall have frequency content between 250 Hz and 4 kHz. Signals may be continuous broad band, continuous discrete tones, stepped tones, tone bursts or impulses.

The minimum recommended frequency resolution is a 1/3 octave band such as might be achieved by use of sound level meters with a band-pass filter.

The use of a spectrum analyzer should lead to a higher frequency resolution (see 5.4).

The sound source shall generate a sound pressure level that is at least 10 dB higher than the ambient sound pressure level in each 1/3 octave band in the frequency range of interest from 250 Hz to 4 kHz. The sound source shall have a smooth free-field frequency response with no significant maxima or minima over the principal frequency range of interest.

It is to be expected that the acoustic impedance of the ground surface will vary with location. Consequently, a sufficient number of measurements shall be taken to establish the variability with position. The source and the receiver shall be translated or rotated, or by both techniques, moved to an adjacent piece of nominally identical ground. A minimum of four independent measurements shall be made for every geometry and location.

The total signal complex sound pressure ratio, $T(f)$ [see Equation (C.1) in Annex C], is obtained by the same procedure for each test location and each geometry.

Ideally, microphones should be selected that have nominally identical pressure sensitivity, nominally identical frequency response, and nominally identical phase response. These characteristics will require extensive calibrations. Despite calibration of the microphones, there will be some relative phase response. It is essential to take account of this for the complex sound pressure ratio method (see 4.5.1, Step 2) by averaging the complex pressure ratios obtained before and after reversing the positions of the upper and lower microphones. This procedure is advisable also when the template method (see 4.5.1, Step 1) only is used.

4.4 Ground and environmental conditions

No acoustical data shall be measured when the average wind velocity exceeds 5 m/s when measured at a height of 2.0 m above the ground. A wind speed of 5 m/s or less is desirable for level difference measurements using two microphones simultaneously. Although use of a single microphone for successive measurements at the two positions is not recommended, it might give reasonable results by the template method (see 4.5.1, Step 1) as long as a more restrictive wind speed limit of 2.5 m/s is observed.

No measurement shall be made during any form of precipitation.

The ground shall be in the condition desired for the measurements. It can be dry, wet, snow covered, frozen, or in any other condition provided that there is an accurate description of it in the test report. If the ground of interest is frequently wet and ground impedance values are needed for this common condition, soil moisture content shall be determined from a moisture-sealed soil sample taken in a representative ground location immediately after the ground impedance measurements. The moisture content may be determined by measuring the percent change in weight of the soil sample, relative to the dry weight, before and after drying it completely in a suitable drying oven. This moisture content shall be included in the test report.

A ground profile that is convex or concave over the test site is not covered by this Standard. Over the distance d (see Figure 1), the test site shall be flat within ± 0.05 m and there should not be any reflecting objects within ten times the separation distance between source and receiver.

Rough ground surfaces with a variation in height of less than 0.05 m may be treated as flat ground for the purpose of this Standard. In the case of sloping ground, the source and microphone heights shall be measured perpendicular to the surface.

NOTE 1 For the purposes of this Standard, reference meteorological conditions are:

Static air pressure	101.325 kPa
Air temperature	288.15 K (15 °C)
Relative humidity	50 %

For these values $\rho_0 c_0 = 416.45 \text{ Pa/(m/s)}$.

The uncertainty in the specific acoustic (characteristic) impedance, ρc of air introduced by differences between the conditions prevailing at the time of measurement and the reference meteorological conditions is not important in comparison to the other uncertainties in determining the normalized specific ground impedance ratio.

NOTE 2 The specific acoustic (characteristic) impedance, ρc of air for any normal range of temperatures, T in Kelvin and Relative Humidity, RH, in %, and at a sea level atmospheric pressure of 1.01325 kPa, can be defined, to an accuracy of better than $\pm 0.2\%$, by: $\rho c = 428.0 / [(T/273.15)^{1/2} (1 + 1.95 \times 10^{-5} \times \text{RH}(\%))]$ Pa/(m/s).

4.5 Determination of the normalized specific acoustic impedance ratio

4.5.1 Steps for obtaining real and imaginary parts of normalized specific acoustic impedance ratio

The real and imaginary parts of the normalized specific acoustic impedance ratio ($Z_s / \rho_0 c_0$) of the ground, henceforth abbreviated to normalized surface impedance, shall be obtained by best fit between measured and calculated level differences using the following four steps:

Step 1 - Template method

The magnitude of the measured level difference spectrum, $LD(f)$ [see Equation (C.3)], shall be compared with that predicted using either (or both) of the two models specified in 4.5.2 and 4.5.3. This Standard provides a set of predicted level difference magnitudes and tables for each of the recommended geometries and for each normalized surface impedance model for use as templates to yield best-fit values of model parameters. Equations (C.1) through (C.9) in Annex C enable the user to calculate level difference spectra for other normalized surface impedance models.

The measured level difference spectrum shall be the average of those measured before and after switching the microphone locations. The difference given by Equation (8) between the measured and calculated $LD(f)$, based on the templates (Figures 3 through 5) or use of Tables 1 through 6 in Clause 9, shall be determined and the parameters for which this difference is minimum shall be found using the procedure set out in 4.6. The impedance spectrum corresponding to the best-fit parameters shall be determined using the appropriate formulae in 4.5.2 and 4.5.3.

Step 2 - Complex sound pressure ratio method

The measured complex sound pressure ratio, $T(f)$ [Equation (C.1)], shall be the arithmetic average of the magnitudes (in dB) and the phases of averaged complex pressure ratios obtained before and after reversing the microphone positions.

The real and imaginary parts of the surface impedance shall be determined at each measured frequency that give the minimum difference between measured and computed complex sound pressure ratio for each of the geometries A and B. An efficient procedure for finding best-fit values is given in Clause 4.7. The procedure shall be repeated for each measurement.

Step 3 - Smoothing (optional)

If a narrow-band spectrum is recorded, the resulting complex normalized surface impedance from Step 2 may be smoothed by a 5-point moving average method. If one-third octaves are used, the resulting impedance spectrum might be sufficiently smooth.

Step 4 - Comparisons

The real and imaginary parts of the normalized surface impedance deduced from each of the geometries shall be plotted on the same axes and validated by comparison with the model-predicted impedance spectrum resulting from Step 1.

4.5.2 One-parameter model

According to this model, and assuming a harmonic time dependence of $e^{-i\omega t}$, the real and imaginary parts of the normalized specific acoustic impedance ratio are respectively given by:

$$\text{Re}(Z_s / \rho_0 c_0) = 1 + 9.08(1000f / \sigma_{\text{eff}})^{-0.75} \quad (1)$$

$$\text{Im}(Z_s / \rho_0 c_0) = 11.9(1000f / \sigma_{\text{eff}})^{-0.73} \quad (2)$$

where f is the frequency and σ_{eff} (in kPa s/m²) is a parameter representing an effective flow resistivity of the ground. Naturally occurring ground surfaces may be expected to have effective flow resistivities in the range 10000 to 30×10^3 kPa s/m². Typical effective flow resistivity values inferred from measured data are tabulated in Annex B for a variety of different ground types.

Templates 1A and 1B show level difference curves calculated for geometries A and B using this one-parameter model with the specified values of effective flow resistivity. The level differences calculated at each one-third octave band center frequency between 250 and 4000 Hz for the specified values of effective flow resistivity are tabulated in the corresponding tables for geometries A and B, respectively. The real and imaginary parts of the normalized acoustic surface impedance ratio are calculated from Equations (1) and (2), respectively, for the value of σ_{eff} that yields the best fit to the measured data.

4.5.3 Two-parameter model

This model is appropriate where ground properties vary with depth. The real and imaginary parts of the normalized specific acoustic impedance ratio are respectively given by:

$$\operatorname{Re}(Z_s / \rho_0 c_0) = \frac{1}{\sqrt{\pi \gamma \rho_0}} \sqrt{\frac{\sigma_e}{f}} \quad (3)$$

$$\operatorname{Im}(Z_s / \rho_0 c_0) = \frac{1}{\sqrt{\pi \gamma \rho_0}} \sqrt{\frac{\sigma_e}{f}} + \frac{c_0 \alpha_e}{4 \pi f} \quad (4)$$

where γ is the ratio of specific heats in air and σ_e (in kPa s/m²) is a parameter representing an effective flow resistivity of the ground (**note that σ_e , while also an effective flow resistivity, is not the same as σ_{eff} , in the one-parameter model**). The additional parameter, α_e (/m), represents an effective rate of change of porosity with depth. Naturally occurring ground surfaces may be expected to have effective flow resistivities, σ_e , in the range 5000 to 30×10^3 kPa s/m². The lower end of this range would be typical of thick, newly fallen snow. The upper end would correspond to compacted fine grain soil. In terms of the two-parameter model the parameter α_e may be expected to vary between 3 and 250 m⁻¹. Typical parameter values inferred from measured data are tabulated in Annex B for a variety of different ground types.

Templates 2A and 2B show level difference curves calculated for geometries A and B using this two-parameter model with specified values of the parameter pair σ_e and α_e , respectively. The level differences calculated at each one-third octave band center frequency between 250 and 4000 Hz using the specified values of the parameter pair are tabulated in the corresponding tables for geometries A and B. The real and imaginary parts of the normalized acoustic surface impedance ratio shall be calculated from Equations (3) and (4), respectively, for the value of the parameter pair σ_e and α_e that yields the best fit to the measured data.

4.5.4 User-defined model

It may not be possible to obtain a good fit between measured and calculated level differences for some grounds when using the templates provided with this Standard. In such cases, either results obtained using the impedance fitting approach (Step 2 of the procedure) may be usable, or the ground type falls outside the scope of the Standard. If the user wishes to calculate custom templates from any impedance model appropriate for naturally occurring grounds information about the required calculations is given in Annexes C and D.

4.6 Procedure to determine best fit in Step 1

For each measurement and each frequency (or frequency band) record the complex sound pressure ratio, T , between the top and bottom microphone.

For each frequency, f , calculate the level difference averaged over n measurements using:

$$LD_{av}(f) = 10 \lg \left(\frac{1}{n} \sum_{j=1}^n |T_j(f)| \right) \quad (5)$$

When the range of values of magnitude of T at each frequency is not greater than 5 dB, a simple arithmetic mean of the level differences may be used for LD_{av} . For such cases:

$$LD_{av}(f) = \frac{1}{n} \sum_{j=1}^n LD_j(f) \quad (6)$$

where LD_j are the individual (measured) level difference measurements at a given frequency.

Then calculate the standard deviation, $\phi(f)$, in decibels, at each frequency using:

$$\phi(f) = \left[\frac{1}{n-1} \sum_{j=1}^n (LD_j(f) - LD_{av}(f))^2 \right]^{1/2} \quad (7)$$

The set of calculated level differences $LD_c(f)$ that produce the best fit to the measured values are those that minimize the value of E given by Equation (8):

$$E = \sum_f \left(\frac{LD_c(f) - LD_{av}(f)}{\phi(f)} \right)^2 \quad (8)$$

where \sum_f indicates a sum over all frequencies. The number of times Equation (8) needs to be calculated can be reduced by first plotting the measured level differences on the corresponding templates and visually eliminating the curves that *obviously* do not correspond to a good fit.

The formulae needed to calculate LD_c are given in Annex C. In the case of the one-parameter model, the normalized specific acoustic impedance ratio of the ground shall be calculated from Equations (1) and (2) using the value of σ_{eff} that minimizes Equation (8). In the case of the two-parameter model, the normalized specific acoustic impedance ratio shall be calculated from Equations (3) and (4) using the parameter pair σ_e and α_e that minimizes Equation (8). Example measurements made above four ground surfaces are reported in Annex A.

4.7 Minimization procedure for Step 2

Although the eventual output of this Standard is the normalized specific acoustic impedance ratio of a ground surface, the quantity deduced in the calculations for Step 2 is the inverse of this *viz.* the normalized specific acoustic admittance. The normalized specific acoustic admittance of the ground surface shall be obtained by an iterative method (the Newton-Raphson method is used in the accompanying software, see Annex E) involving the measured and calculated complex sound pressure ratios between two microphones. The process shall be repeated for each measurement. It is recommended that the complex sound pressure ratios determined from repeated measurements for a given geometry be averaged and that obviously incorrect ones be discarded before the normalized specific acoustic impedance ratio is calculated.

Start at the lowest frequency with an admittance value (x_0) of $0.0 + i0.0$ corresponding to perfectly reflecting ground. The complex admittance of the ground surface under investigation is the value giving the best fit between measured complex sound pressure ratio, T_m , and the computed value, T .

In the Newton-Raphson method, a 'better' approximation, say x_{n+1} , to specific admittance can be obtained from:

$$x_{n+1} = x_n - \frac{T(x_n) - T_m}{\left[dT(x_n)/d\beta \right]_{\beta=x_n}} \quad (9)$$

where x_n is the initial ($n = 0$) or a previous approximation for the admittance. This Equation shall be applied to each frequency value starting from the lowest frequency.

Annex C gives the formulae for sound pressure at each microphone, L , the complex sound pressure ratio, T , and the derivative of T with respect to the surface admittance, β .

A final solution is obtained by iterating Equation (9) until a desired accuracy is achieved. The suggested tolerance is 0.1% i.e. $|x_{n+1} - x_n|/|x_n| < 0.001$. Normally 10 iterations are sufficient to achieve this accuracy. The starting value of the normalized specific acoustic admittance shall be (0.0+ j 0.0) for the lowest frequency. Thereupon the value arrived at for the previous (lower) frequency shall be the starting value for the next frequency point.

The number of iterations shall not exceed 100. In the event of failing to achieve the desired accuracy by 100 iterations, the calculation shall be stopped and the value for that frequency point assumed void.

Expressions for both the reflection coefficient and the derivative term can be evaluated quickly by series expansion given in standard mathematical textbooks. The user is referred to Annex D for an algorithm to evaluate $W(z)$ for complex z .

5 Required instruments for measuring ground impedance outdoors

5.1 Sound source

Within the frequency range of interest, the sound source shall satisfy classical inverse square law theory and be omnidirectional to within 1 dB within $\pm 45^\circ$ both in the vertical and horizontal planes.

A sound source that satisfies the directional requirements consists of a driver feeding into one end of a pipe with a diameter no more than $\lambda/4$, where λ is the wavelength. The other end of the pipe acts as a point source that obeys classical theory for radiation from a pipe. A convenient method for constructing such a source is to use a compression driver furnished with screw threads to which, normally, a horn is attached. The horn should be replaced by a brass tube of length no less than 0.5 m and diameter no more than 0.03 m [1]. An example of such a device is shown in Figure 2.



Figure 2 – Point source and vertically separated microphones at the Open University, UK

5.2 Microphones

Microphone characteristics shall conform to the requirements of IEC 61672-1.

Microphones shall be calibrated prior to measurements.

The orientation should be for normal incidence.

All items used to hold or support microphones shall be oriented so as to produce minimum shielding or reflection of noise from the source to the microphone.

High humidity or temperature will change the sensitivity or damage many types of microphones. The microphone manufacturer's instructions shall be carefully followed to avoid such effects.

5.3 Calibration

A microphone calibrator with an accuracy of ± 0.5 dB, meeting the requirements of ANSI S1.40, shall be used.

Calibration checks shall be performed at least at the beginning and end of each measurement session.

5.4 Sound level meter/analyzer

Measurement systems shall meet the requirements of IEC 61672-1.

Frequency filter sets, if used, shall meet the requirements of ANSI/ASA S1.11.

The minimum instrumentation for executing the template method (see 4.5.1, Step 1) is a single sound level meter and one-third octave band frequency filters, subject to constraints on the permissible variation in atmospheric conditions between measurements (see 4.4). The availability of two sound level meters and filter sets can improve the ability to carry out the template method as long as measurements are made before and after the positions of the microphones are reversed and the results are averaged (see also 4.3). A two-channel signal processing system capable of frequency and phase analysis is required to carry out the complex sound pressure ratio method

(see 4.5.1, Step 2). The frequency response of the measurement system shall be calibrated at least annually to conform to the specifications of IEC 61672-1.

5.5 Miscellaneous

A windscreen meeting microphone manufacturer's recommendations shall be used on each microphone during measurements if the wind speed measured by the anemometer exceeds 1 m/s.

For general guidance on all other issues pertaining to instrumentation for the measurement of sound pressure level, see ANSI S1.13.

5.6 Configuration of measuring system

The measuring system, including the operator, shall be positioned in such a way that it does not contribute to the measured levels (refer to 4.4).

5.7 Wind speed

An anemometer or other device for measuring wind speed and direction shall be used. This device shall have an accuracy of $\pm 10\%$ of full scale or better. An averaging time of 10 to 20 s is desirable. The device shall be mounted at a height of 2 m.

6 Measurement

Background sound pressure levels and wind speed need to be monitored and the measurement shall be conducted only if these variables fall within the predetermined limits (see section 4.4).

6.1 Area of ground

The measurements shall be made above different locations within the area of interest to get an area-average. The area representing the ground surface under measurement shall be determined by visual inspection. It is advisable to include a photograph of this area with the report. See also 4.4 concerning the possible need to obtain soil samples for moisture content data.

6.2 Data collection

6.2.1 Initial and final calibration

Calibrate equipment per the manufacturer's instruction, with all cabling to be used in the measurement in the circuit for calibration and electrical interference checks.

Perform a final calibration check for all microphones. Changes in calibration exceeding 1 dB are unacceptable. In such cases, equipment should be checked, and measurements made at microphones showing such a shift shall be discarded and repeated. Changes in calibration of less than 1 dB may be accounted for.

6.2.2 Meteorological

Temperature, relative humidity, and wind speed shall be obtained from on-site sensors or from the nearest meteorological office.

The background sound pressure level should be sampled at the microphone positions (see also 4.3).

7 Data reduction

7.1 Corrections

7.1.1 Correction for changes in calibration

If the final calibration level for a sound measuring system differs from the initial calibration level by 1 dB or less, all measurements made with that system shall be adjusted by one-half of the difference (e.g., if the final level is lower than the initial value, then increase the measured levels).

7.1.2 Correction for excessive background sound

If, compared to the background sound pressure level alone, the increase in the sound pressure level in any given band, with the source operating, is more than 10 dB, the sound pressure level resulting from both the source and background sound is essentially the sound pressure level resulting from the source alone. This is the preferred condition but is frequently unattainable in the field.

If, compared to the background sound pressure level, the increase in sound pressure level in any given band, with the sound source operating, is 10 dB or less, the sound pressure level resulting from the sound source and the background sound pressure level cannot be properly separated with the measuring techniques described in this Standard.

For those cases where the difference is less than 10 dB, the unadjusted source level is to be reported and identified as “masked” by the background level.

7.2 Experimental error

The experimental error is an accumulation of random and bias errors resulting from:

- 1) Instrumentation error (analyzer);
- 2) Variation in levels resulting from changes in wind velocity within the allowable range for a set of measurements;
- 3) Variation in levels within a given cloud cover, or resulting from temperature changes within the prescribed limits;
- 4) Variation in levels resulting from changes in source characteristics within the allowable ranges.

Random errors are estimated by the repetition of the measurements for each source-receiver pair and the resultant computation of a variance for the measurements.

Bias errors include:

- 1) Site bias;
- 2) Errors inherent in prediction model.

8 Reporting

8.1 Introductory information

Documentation shall be sufficiently complete to permit independent repetition of the standard procedure. This will take into account changes in environmental conditions.

8.2 Documentation of the instrumentation

The manufacturer, type, and serial number of all microphones, analyzers, acquisitions system, calibrators, and meteorological sensors shall be reported and keyed to specific measurement points. Settings of controllable instrument parameters such as amplifier gains, recording speeds, recorder gains, field calibration levels, and calibration signal levels and spectra should be provided. Documentation of field calibration shall be included. When data reduction is done away from the site (such as in analyzing tape recordings), documentation of the instrumentation and procedures shall be provided.

8.3 Meteorological data

Data from meteorological sensors shall be reported including average wind velocity, temperature, and humidity. The cloud cover shall also be specified, with a brief statement as to the existing weather conditions.

8.4 Impedance values

The real and imaginary parts of the normalized specific acoustic impedance ratio v. frequency shall be tabulated for the area of ground identified according to 6.1.

8.5 Other observations

A discussion of any unforeseen events during the measurements that could relate to the source emission, sound propagation, or background sound should be included. Any situations that suggest modifications to the experiment for improved results should be documented. Any relevant subjective judgments or interpretations may appear in this section of the measurement report.

9 Templates for obtaining normalized surface impedance model parameters

9.1 Templates for the one-parameter impedance model

Table 1 – Template 1A—Pre-calculated level differences (dB) for geometry A using the one-parameter model

Freq. (Hz)	Effective flow resistivity, σ_{eff} kPa s/m ²							
	10	32	63	100	160	320	1000	3200
250	0.3	-1.1	-1.1	-1.0	-0.9	-0.8	-0.7	-0.7
315	0.4	-1.3	-1.4	-1.4	-1.3	-1.2	-1.0	-1.0
400	1.7	-1.4	-2.0	-2.0	-2.0	-1.8	-1.6	-1.5
500	2.8	-0.6	-2.6	-3.0	-3.0	-2.7	-2.5	-2.4
630	3.4	1.7	-1.9	-4.0	-4.9	-4.8	-4.3	-4.0
800	3.3	3.4	1.9	-1.0	-4.9	-8.6	-8.6	-7.6
1000	2.7	3.5	4.1	3.9	2.0	-3.4	-12.7	-18.7
1250	1.4	2.5	3.7	4.9	6.2	6.2	0.9	-2.6
1600	-1.4	-0.1	1.5	2.9	4.7	8.3	13.0	10.1
2000	-5.9	-4.0	-2.3	-0.8	0.9	3.9	10.0	17.2
2500	-4.4	-5.1	-5.5	-5.6	-5.3	-3.6	0.4	3.7
3150	1.6	0.9	-0.1	-0.7	-1.7	-3.6	-7.8	-12.6
4000	2.9	2.8	2.6	2.6	2.2	1.7	0.8	0.1

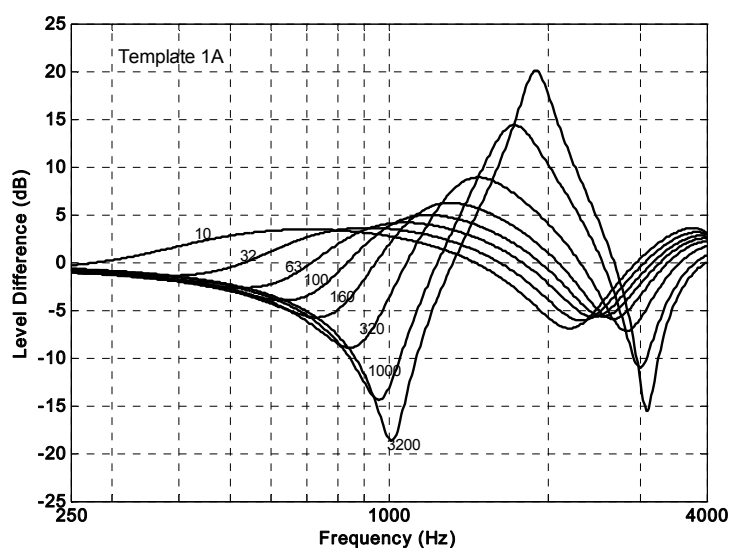


Figure 3a – Template curves for geometry A and eight values of effective flow resistivity, σ_{eff} , between 10 and 3200 kPa s/m²

Table 2 – Template 1B—Pre-calculated level differences (dB) for geometry B using the one-parameter model

Freq. (Hz)	Effective flow resistivity, σ_{eff} kPa s/m ²							
	10	32	63	100	160	320	1000	3200
250	−0.8	0.9	−0.7	−0.6	−0.5	−0.4	−0.3	−0.3
315	−0.7	−1.1	−0.9	−0.8	−0.7	−0.6	−0.4	−0.4
400	0.3	−1.3	−1.3	−1.1	−1.0	−0.8	−0.6	−0.5
500	0.6	−1.5	−1.6	−1.5	−1.3	−1.1	−0.9	−0.8
630	2.1	−1.3	−2.1	−2.1	−1.9	−1.6	−1.3	−1.1
800	4.0	−0.1	−2.4	−2.9	−2.8	−2.5	−2.0	−1.7
1000	5.6	2.2	−1.4	−3.4	−4.1	−3.8	−3.1	−2.7
1250	6.8	4.8	1.4	−1.8	−4.7	−6.0	−5.1	−4.5
1600	7.4	6.8	5.1	2.6	−1.2	−7.2	−9.8	−8.5
2000	7.2	7.4	7.1	6.1	3.8	−1.6	−11.8	−18.2
2500	6.0	6.7	7.2	7.4	7.0	4.4	−2.6	−7.6
3150	3.2	4.2	5.3	6.2	7.2	7.8	4.0	−0.3
4000	−2.6	−1.1	0.4	1.8	3.5	6.5	8.0	4.9

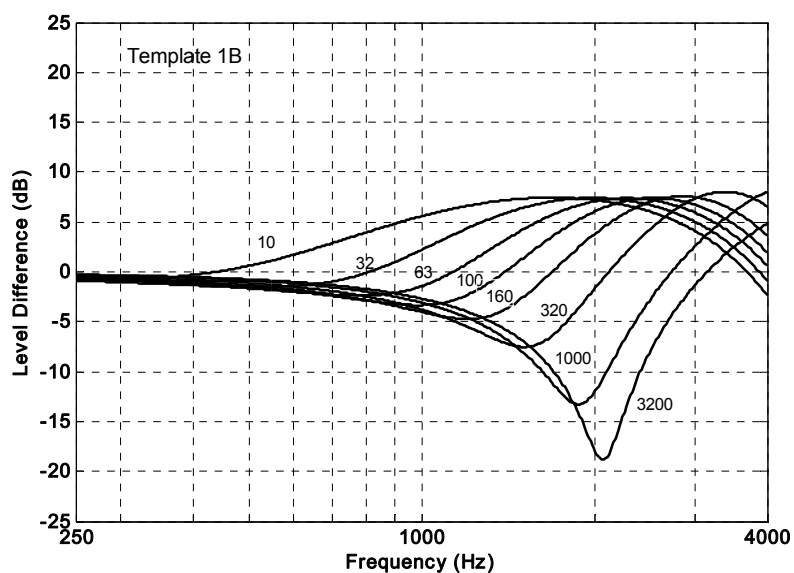


Figure 3b – Template curves for geometry B and eight values of effective flow resistivity, σ_{eff} , between 10 and 3200 kPa s/m²

9.2 Templates for the two-parameter normalized surface impedance model

The template tables and figures for the two-parameter model each use a stated value for the effective rate of change of porosity with depth parameter, α_e , but three values for the effective flow resistivity, σ_e .

Table 3 – Template 2A—Pre-calculated level differences (dB) for geometry A using the two-parameter model

Freq. (Hz)	Effective flow resistivity, σ_e kPa s/m ²						
	$(\alpha_e = 3 \text{ m}^{-1})$				$(\alpha_e = 50 \text{ m}^{-1})$		
	10	32	100	1000	10	100	1000
250	-1.3	-1.0	-0.9	-0.7	-1.3	-0.9	-0.7
315	-1.7	-1.4	-1.2	-1.0	-1.9	-1.2	-1.0
400	-2.2	-2.1	-1.8	-1.6	-2.9	-1.9	-1.6
500	-1.9	-3.1	-2.8	-2.4	-4.8	-2.9	-2.4
630	1.6	-4.3	-4.7	-4.1	-7.1	-5.0	-4.1
800	5.3	-1.2	-7.5	-8.0	4.7	-9.0	-8.0
1000	5.3	4.7	-2.0	-14.7	9.1	-3.2	-15.1
1250	4.0	6.1	6.4	-1.2	6.2	7.0	-1.2
1600	1.2	3.9	7.9	11.0	2.7	9.2	11.1
2000	-4.0	-0.3	3.8	13.4	-2.4	4.4	13.6
2500	-8.7	-7.5	-3.7	2.9	-10.7	-3.6	2.9
3150	0.4	-1.5	-4.1	-11.2	-0.3	-4.6	-11.3
4000	4.1	2.8	1.7	0.2	3.9	1.6	0.2
	$(\alpha_e = 100 \text{ m}^{-1})$				$(\alpha_e = 250 \text{ m}^{-1})$		
	10	100	1000		10	100	1000
250	-1.1	-0.9	-0.7		-0.8	-0.8	-0.7
315	-1.6	-1.2	-1.0		-1.2	-1.2	-1.0
400	-2.5	-1.9	-1.6		-2.0	-1.8	-1.6
500	-4.2	-2.9	-2.4		-3.2	-2.8	-2.4
630	-8.4	-5.0	-4.1		-5.7	-4.8	-4.1
800	-4.7	-10.0	-8.0		-16.0	-10.3	-8.1
1000	13.3	-4.7	-15.6		-1.2	-9.2	-16.9
1250	9.1	7.0	-1.3		20.6	5.2	-1.7
1600	4.2	10.6	11.2		9.0	15.2	11.3
2000	-1.0	5.0	13.9		2.0	6.8	14.7
2500	-11.8	-3.4	2.9		-9.5	-2.5	3.1
3150	-1.0	-5.0	-11.5		-3.0	-6.3	-12.0
4000	36.0	1.5	0.2		2.8	1.3	0.1

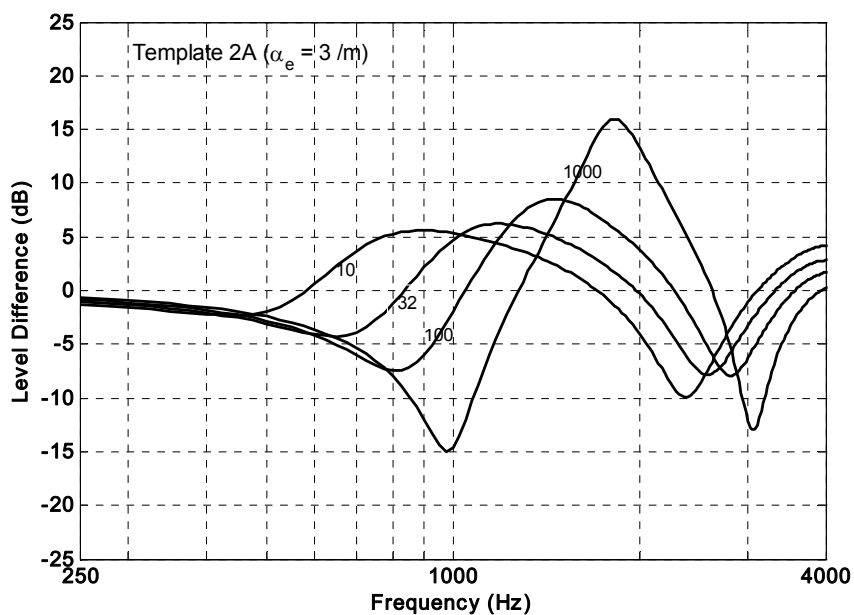


Figure 4a – Template curves for geometry A with $\alpha_e = 3/m$ and four values of effective flow resistivity, σ_e (10, 32, 100, and 1000 kPa s/m²)

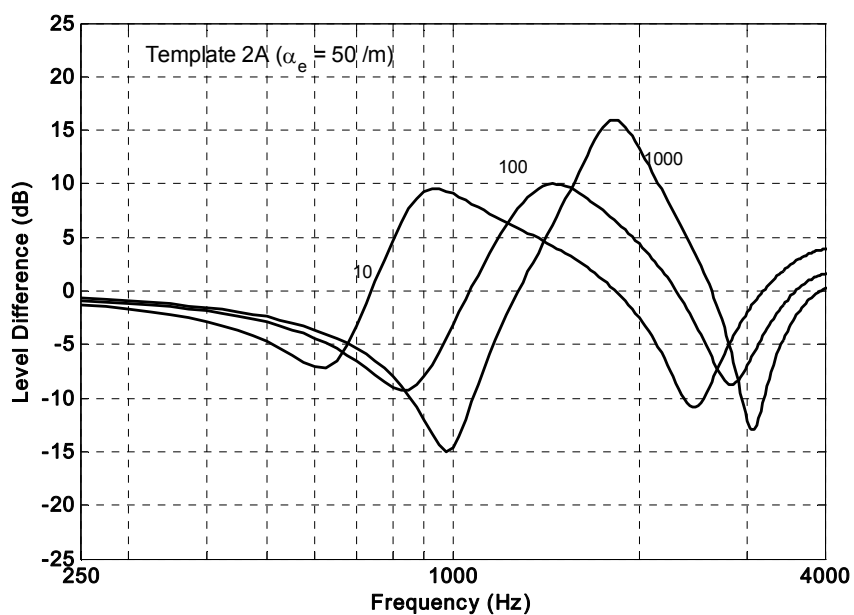


Figure 4b – Template curves for geometry A with $\alpha_e = 50/m$ and three values of effective flow resistivity, σ_e (10, 100, and 1000 kPa s/m²)

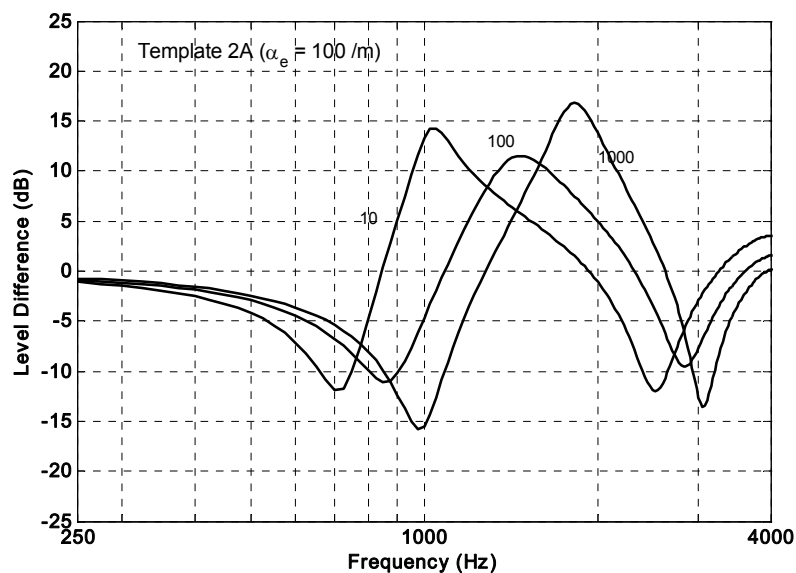


Figure 4c – Template curves for geometry A with $\alpha_e = 100/m$ and three values of effective flow resistivity, σ_e (10, 100, and 1000 kPa s/m²)

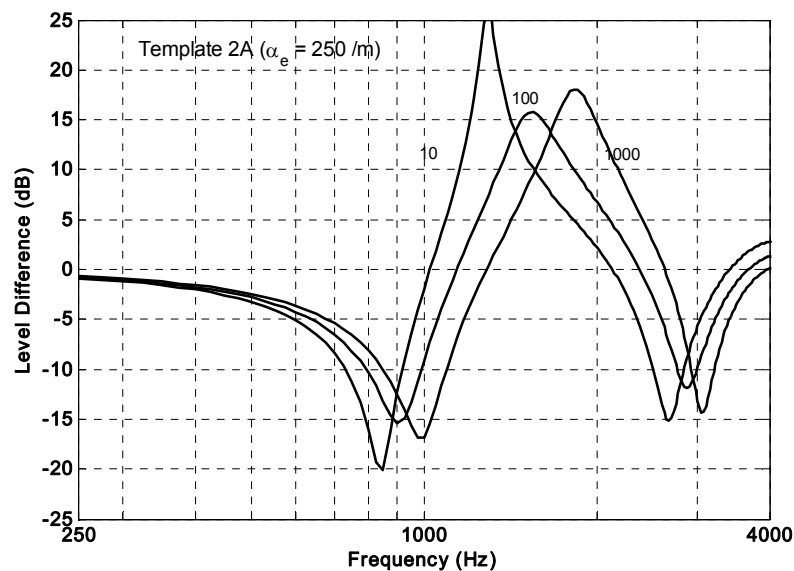


Figure 4d – Template curves for geometry A with $\alpha_e = 250/m$ and three values of effective flow resistivity, σ_e (10, 100, and 1000 kPa s/m²)

Table 4 – Template 2B—Pre-calculated level differences (dB) for geometry B using the two-parameter model

Freq. (Hz)	Effective flow resistivity, σ_e kPa s/m ²						
	$(\alpha_e = 3 \text{ m}^{-1})$				$(\alpha_e = 50 \text{ m}^{-1})$		
	10	32	100	1000	10	100	1000
250	-1.0	-0.6	-0.5	-0.3	-0.8	-0.5	-0.3
315	-1.3	-0.8	-0.6	-0.4	-1.2	-0.6	-0.4
400	-1.7	-1.2	-0.9	-0.6	-1.7	-0.9	-0.6
500	-2.3	-1.6	-1.2	-0.8	-2.4	-1.2	-0.8
630	-2.9	-2.2	-1.7	-1.2	-3.5	-1.7	-1.2
800	-2.7	-3.2	-2.6	-1.8	-5.6	-2.6	-1.9
1000	0.7	-4.3	-3.9	-2.8	-7.7	-4.0	-2.9
1250	6.0	-3.5	-5.9	-4.7	-1.1	-6.5	-4.7
1600	10.2	2.0	-6.7	-8.8	9.6	-8.4	-8.8
2000	11.3	7.3	-1.2	-15.1	13.4	-2.3	-15.5
2500	10.0	10.0	4.8	-5.8	12.2	4.4	-5.9
3150	6.9	9.0	8.8	1.3	8.6	9.2	1.3
4000	0.3	4.0	8.0	5.8	1.2	8.9	5.8
	$(\alpha_e = 100 \text{ m}^{-1})$				$(\alpha_e = 250 \text{ m}^{-1})$		
	10	100	1000		10	100	1000
250	-0.7	-0.5	-0.3		-0.4	-0.4	-0.3
315	-0.9	-0.6	-0.4		-0.6	-0.5	-0.4
400	-1.4	-0.9	-0.6		-0.9	-0.8	-0.6
500	-2.0	-1.2	-0.8		-1.4	-1.1	-0.8
630	-3.0	-1.7	-1.2		-2.1	-1.6	-1.2
800	-4.9	-2.6	-1.8		-3.3	-2.5	-1.9
1000	-8.6	-4.1	-2.9		-5.5	-3.9	-2.9
1250	-9.9	-6.7	-4.7		-10.7	-6.6	-4.7
1600	4.9	-10.2	-8.9		-12.2	-13.1	-8.9
2000	14.2	-3.6	-15.9		3.0	-7.4	-17.0
2500	14.9	3.9	-6.0		16.9	1.8	-6.3
3150	10.2	9.4	1.2		17.7	8.9	1.0
4000	3.4	9.9	5.7		7.9	12.3	5.7

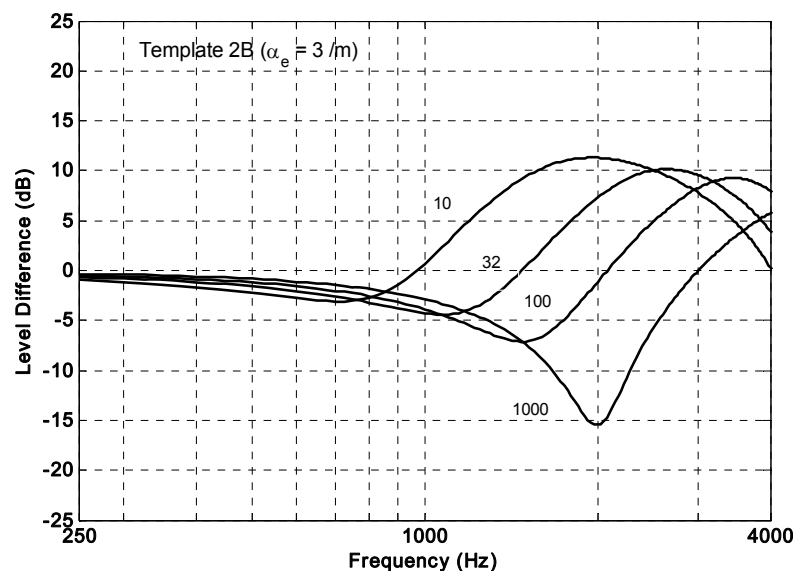


Figure 5a – Template curves for geometry B with $\alpha_e = 3/m$ and four values of effective flow resistivity, σ_e (10, 32, 100, and 1000 kPa s/m²)

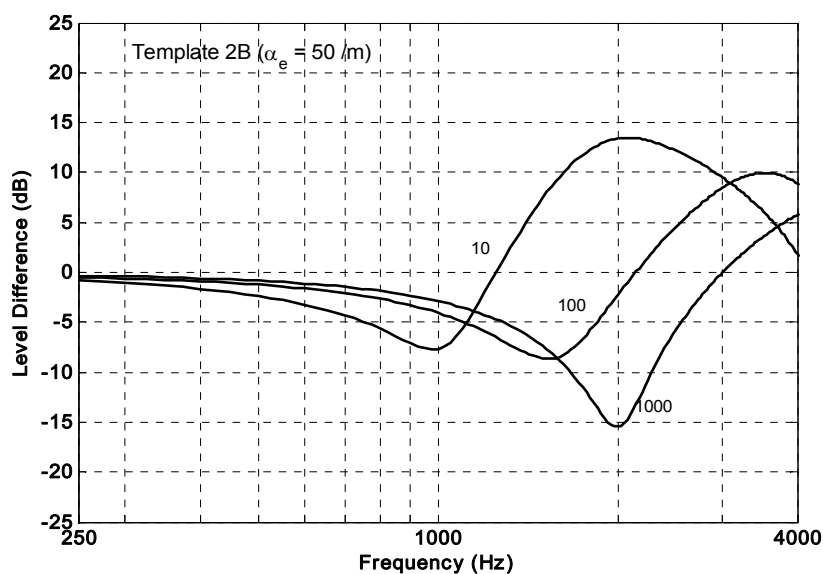


Figure 5b – Template curves for geometry B with $\alpha_e = 50/m$ and three values of effective flow resistivity, σ_e (10, 100, and 1000 kPa s/m²)

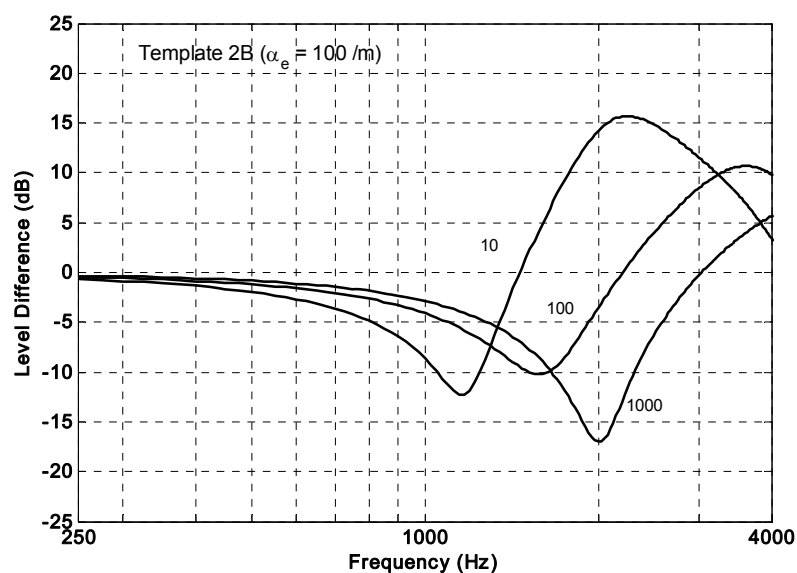


Figure 5c – Template curves for geometry B with $\alpha_e = 100/\text{m}$ and three values of effective flow resistivity, σ_e (10, 100, and 1000 kPa s/m^2)

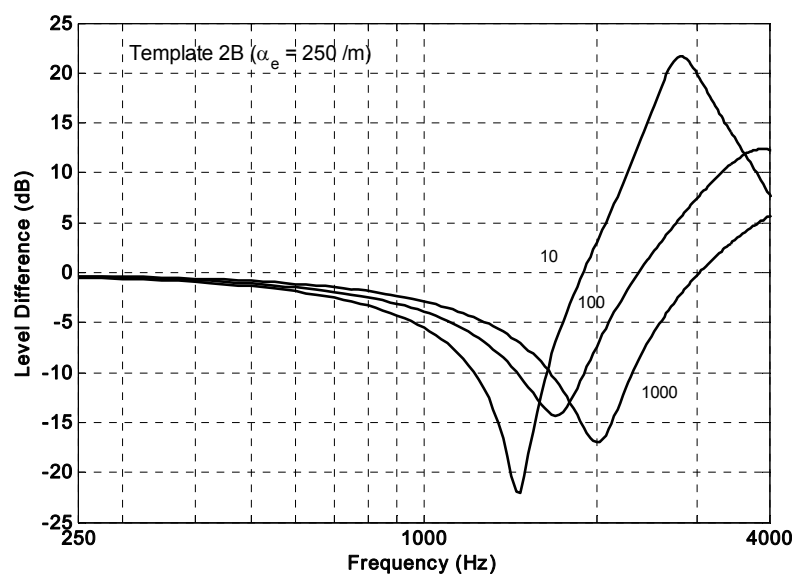


Figure 5d – Template curves for geometry B with $\alpha_e = 250/\text{m}$ and three values of effective flow resistivity, σ_e (10, 100, and 1000 kPa s/m^2)

Annex A

(informative)

Worked examples of procedure

A.1 Example 1: Cricket field at the Open University, UK

Sound Pressure Level Difference (LD) spectra were obtained with source-receiver geometries A and B using a two-channel FFT analyzer. Between four and ten measurements of LD spectra were made with the first microphone arrangement. Then the microphone positions were switched and a similar number of LD measurements were made. Data shown were taken at different areas of the cricket pitch on each of the two measurement days which were four weeks apart. The data at the location referred to as Area 3 were taken first while those labeled Area 1 and Area 2 were taken on a later date. Area 3 was very close to Area 1.

Temperature = 22°C, wind speed between 1.3 and 2.0 m/s.

Step 1

The LD values (in dB) taken at each ground area were averaged and the standard deviations were computed. The resulting data (thick continuous lines with two-standard-deviation error bars at one-third octave intervals correspond to Area 1 (red), Area 2 on day 2 (blue), and Area 3, close to Area 1, on day 1 (black) respectively were superimposed on template plots (see Figure A.1).

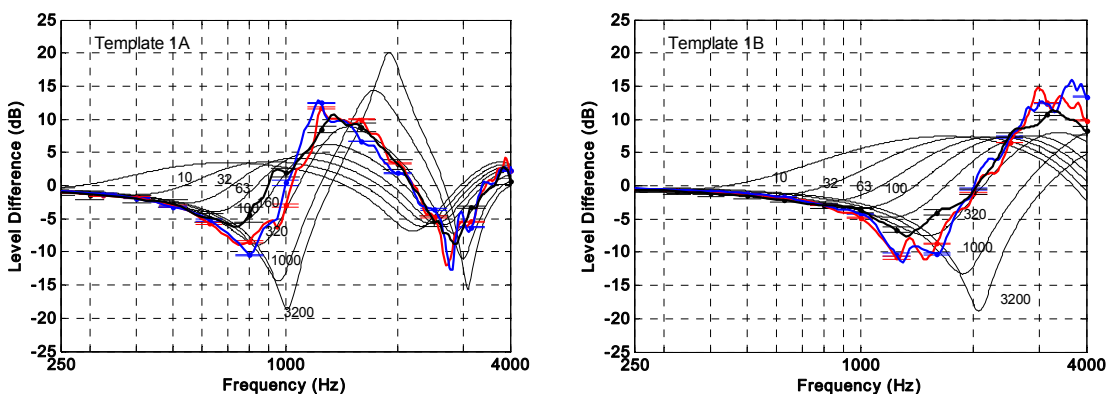


Figure A.1 – Template plots for one-parameter impedance model

The measured level difference spectra do not fit any of the one-parameter template curves particularly well but $\sigma_{eff} = 320 \text{ kPa s/m}^2$ seems to provide the closest fit (see Table A.1).

Table A.1 – Cumulative error, E , for the one-parameter templates, computed using Equation (8) in 4.6

Parameter: σ_{eff} (kPa s/m ²)	160	320	1000
Geometry A			
Area 1	9044	2442	20930
Area 2	17000	14170	90000
Area 3	302.5	194	2336
Geometry B			
Area 1	35000	24000	>100000
Area 2	15000	6700	23000
Area 3	516	368	3414

Plots of data on the templates for the two-parameter model are shown in Figures A.2 (a) through (h):

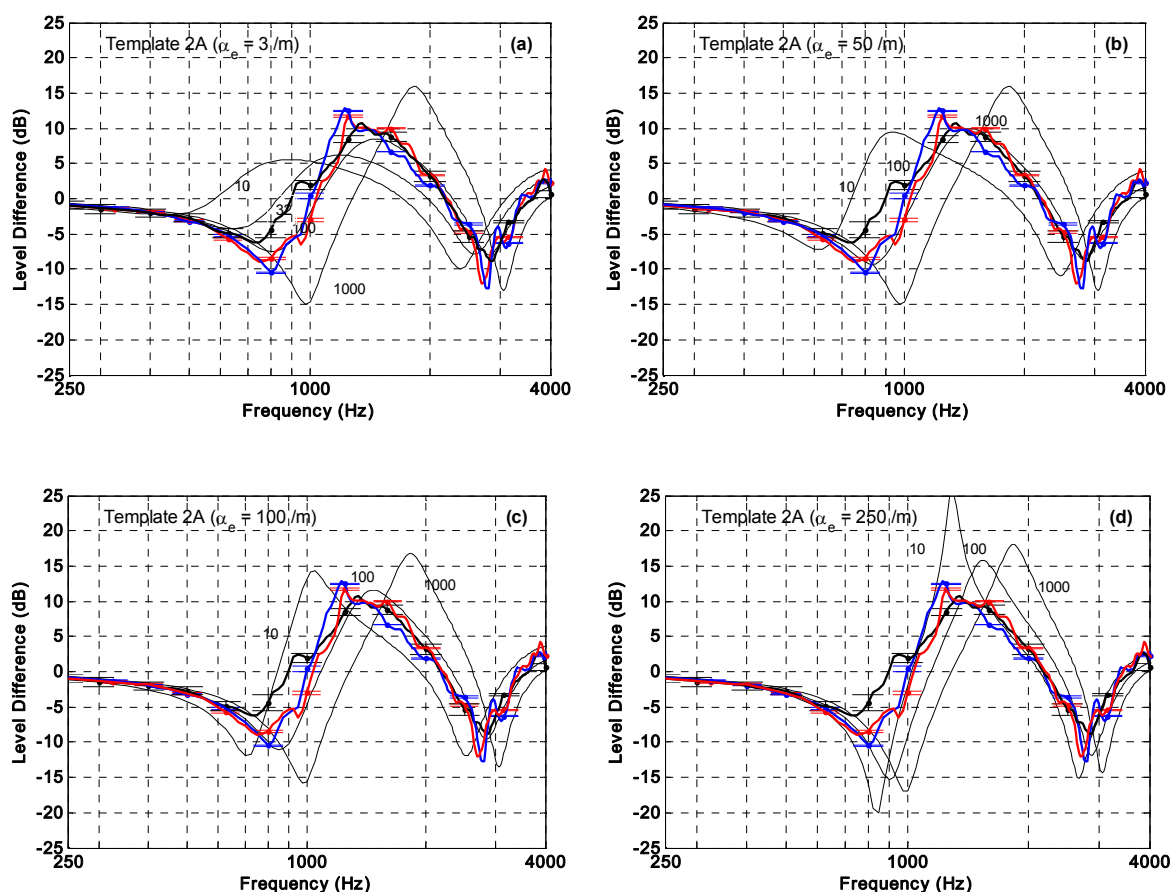


Figure A.2 – Comparisons of measured LD spectra with two-parameter model templates

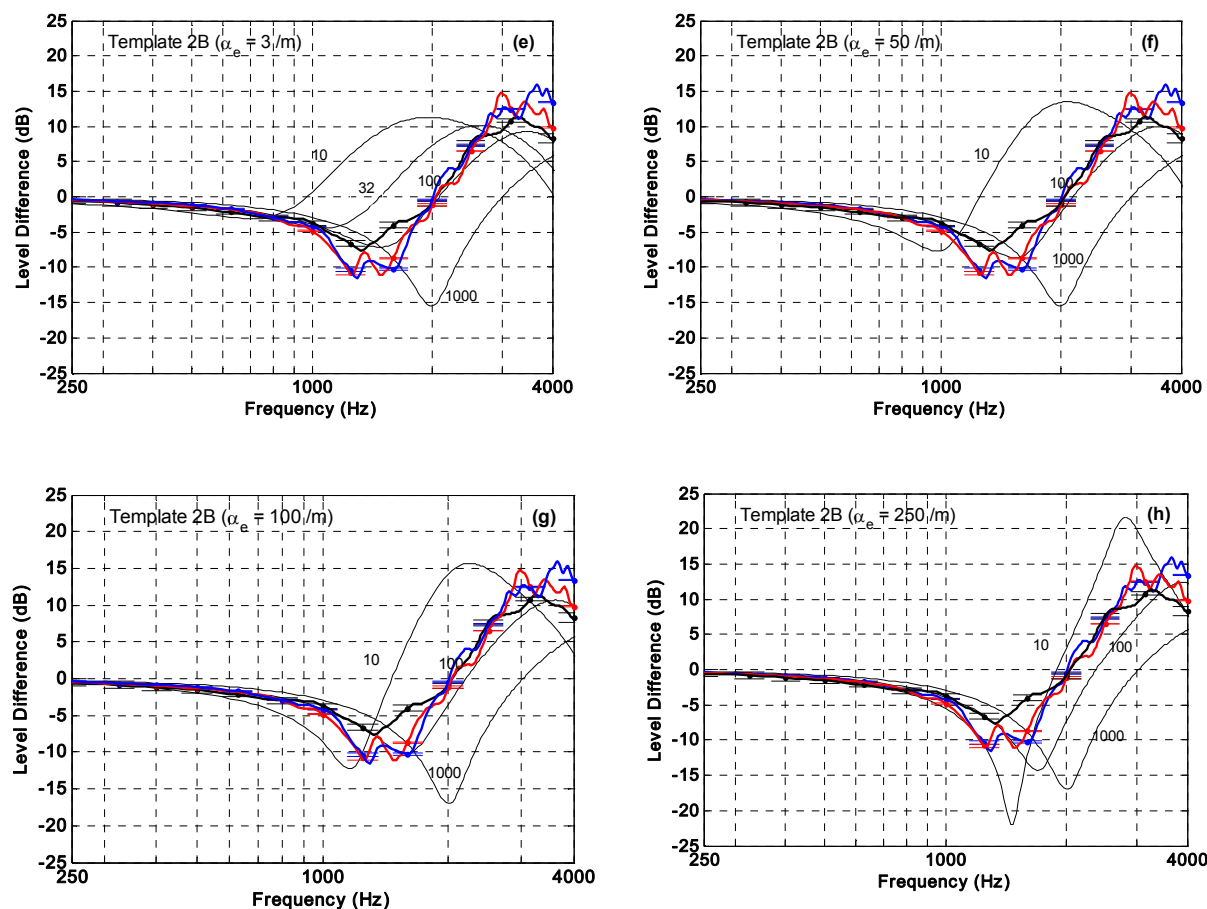


Figure A.2 (continued) – Comparisons of measured LD spectra with two-parameter model templates

Best-fit cumulative error, E , values [Equation (8)] are given in Table A.2 below. There is little to choose between values of 3 and 50 for the second parameter (α_e) in both geometries. Note that the magnitude of cumulative error values is a relative rather than absolute indicator of fit since it depends on the standard deviation of the data at the various frequencies of interest. Some large values of cumulative error nevertheless include small standard deviations at some frequencies.

Table A.2 – Cumulative error, E , for the two-parameter templates, computed using Equation (8) in 4.6

Parameter: σ_e (kPa s/m ²); a_e (/m)	100; 3.0	100; 50.0	100; 100.0
Geometry A			
Area 1	2000	1370	1700
Area 2	11000	16500	29000
Area 3	142	196	300
Geometry B			
Area 1	212	330	560
Area 2	4800	3400	3000
Area 3	516	368	3414

Step 2

Six normalized surface impedance spectra (real and imaginary parts) representing each of the two geometries at each of three test areas, deduced by the method outlined in Step 2, are shown in Figure A.3. They indicate a large variation at low frequencies for the reactance (imaginary part). The solid lines represent deductions using geometry A and the broken lines are for geometry B. The most outlying curves, i.e., highest and lowest reactance values, are from geometry A at the second test area (area 2). The arithmetic means of the six pairs of curves are computed and shown in the same plot as dotted lines.

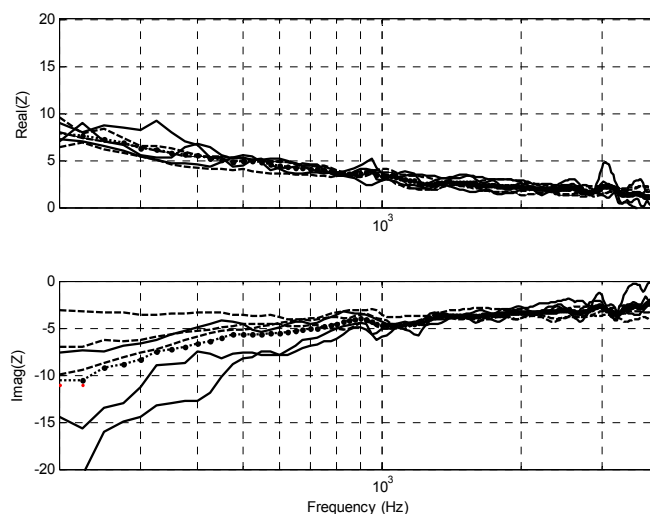


Figure A.3 – Normalized specific acoustic impedance ratio deduced from six sets of averaged complex sound pressure ratios. Those deduced from geometry B are plotted as broken lines. The mean values are plotted as dotted lines.

Step 3

The predicted impedance spectra from Step 2 are sufficiently smooth that 5-point smoothing is not required.

Step 4

Figure A.4 shows the normalized surface impedance ratio spectra predicted by Steps 1 and 2. The broken line is the average from Figure A.3 and solid lines are the best fit one-parameter (asterisks) and two-parameter (dots) models from Tables A.1 and A.2. The two-parameter model agrees better with the averaged deduced impedance from Step 2. The open circles represent a best fit of the two-parameter model to the impedance spectra deduced by the complex sound pressure ratio method (Step 2). This uses values of $\sigma_e = 70 \text{ kPa s/m}^2$ and $\alpha_e = 25 \text{ /m}$. The corresponding cumulative error, E , for the level difference using area 3 data is 142 (in Table A.2).

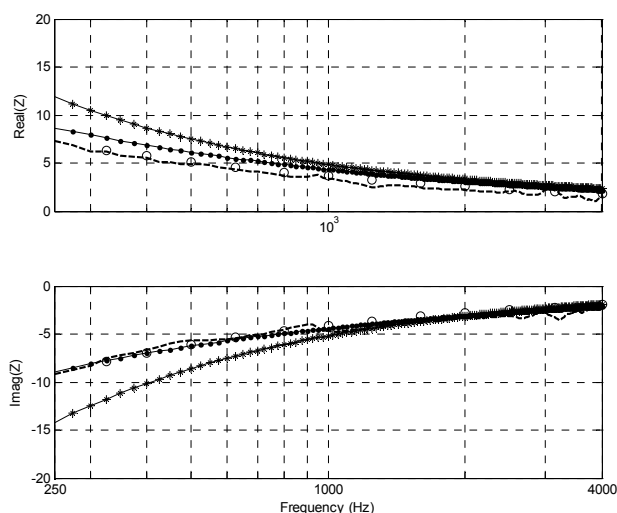


Figure A.4 – A comparison of normalized specific acoustic impedance ratio spectra deduced from Steps 1 and 2 (broken line)

Data obtained using a single microphone

A further set of measurements was recorded at area 1 using a single microphone placed successively at the upper and lower microphone positions. The level difference was computed by dividing the complex spectrum recorded at the upper position by that recorded at the lower position. The measurement was repeated three times. The variation in the phase of the computed complex sound pressure ratio was too large to deduce the normalized specific acoustic impedance ratio by the complex sound pressure ratio method (Step 2). However, it is still possible to use the template method (Step 1). The results are shown in Figures A.5 (a) and (b) for geometry B only. The error bars in the data are larger than those shown in Figures A.1 and A.2, but the conclusions about the best-fit template curves are the same.

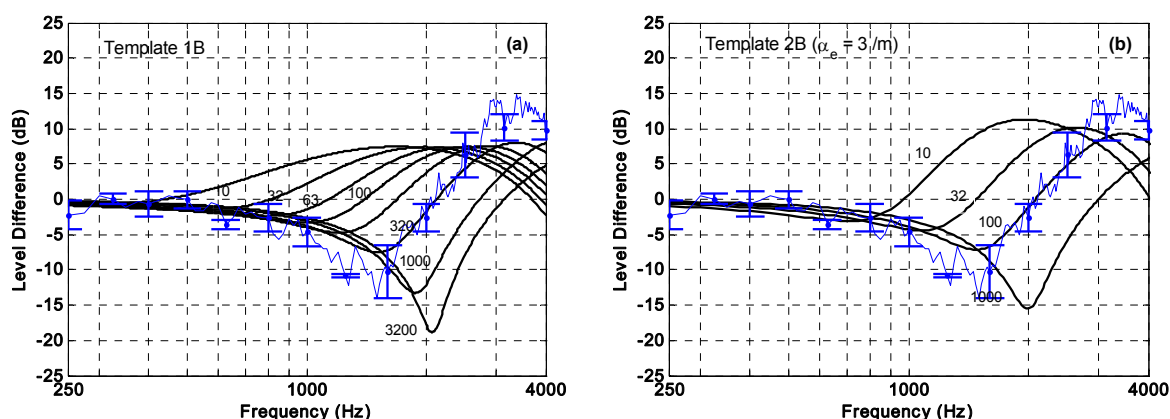


Figure A.5 – Template method (Step 1) using data obtained with a single microphone

A.2 Example 2: Institutional grass at the National Research Council, Canada

Sound level measurements were taken using a point source (compression driver feeding into one end of a pipe) and two B&K ½-inch microphones. The test signal was a stepped sine-sweep (1024 frequencies) and the measured levels were recorded simultaneously on an analyzer and saved as ASCII files. Wind speed was < 1 m/s during the measurements.

Step 1 - Template method

The level differences (LD) were determined for each set of measurements and the average and standard deviations were then computed. The average LD and standard deviation are plotted in Figures A.6 and A.7 for both geometries on the one-parameter template.

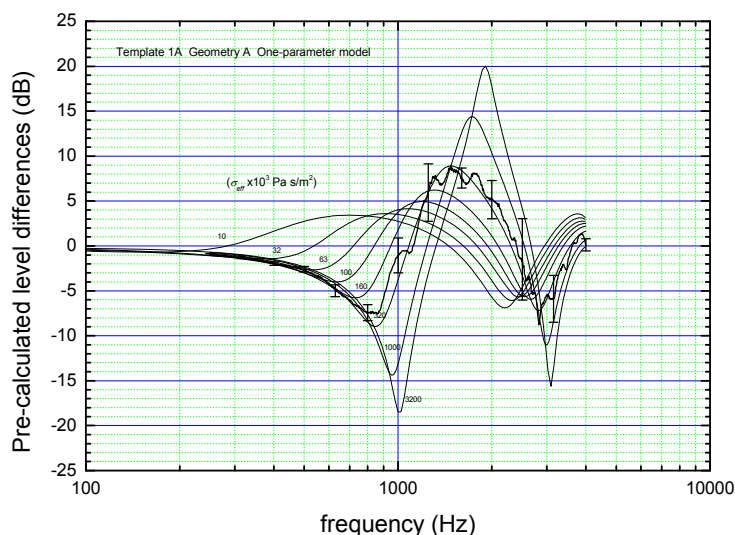


Figure A.6 – Template for geometry A and the one-parameter model with superimposed NRC data

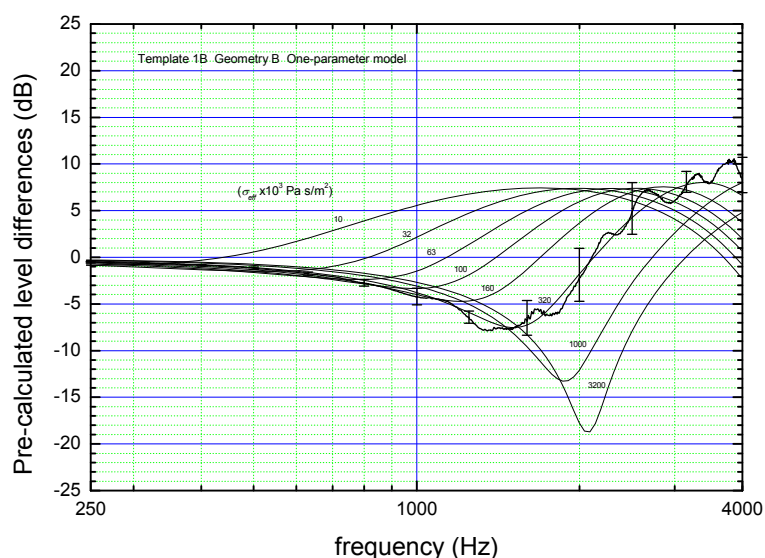


Figure A.7 – Template for geometry B and the one-parameter model with superimposed NRC data

The cumulative errors are shown in Table A.3.

Table A.3 – Cumulative error, E , for the one-parameter templates, computed using Equation (8) in 4.6

Parameter (σ_{eff})	160 000	320 000	1 000 000
Geometry A	3053	773	7250
Geometry B	6610	940	8362

The best fit in both cases are the curves for $\sigma_{eff} = 320 \text{ kPa s/m}^2$.

The data is plotted on the template for the two-parameter model in Figures A.8 and A.9. The cumulative errors are shown in Table A.4.

Table A.4 – Cumulative error, E , for the two-parameter templates, computed using Equation (8) in 4.6

$\alpha_e = 3/\text{m}; \sigma_e \text{ kPa s/m}^2$	32	100	1 000
Geometry A	8848	376	8921
Geometry B	6610	940	8362
$\alpha_e = 50/\text{m}; \sigma_e \text{ kPa s/m}^2$	10	100	1 000
Geometry A	36 944	835	9377
Geometry B	97 882	520	13 155

For geometry A data best fit is obtained for $\alpha_e = 3 \text{ m}^{-1}$ and $\sigma_e = 100 \text{ kPa s/m}^2$, but, for geometry B data, a better fit is obtained for $\alpha_e = 50 \text{ m}^{-1}$ and $\sigma_e = 100 \text{ kPa s/m}^2$.

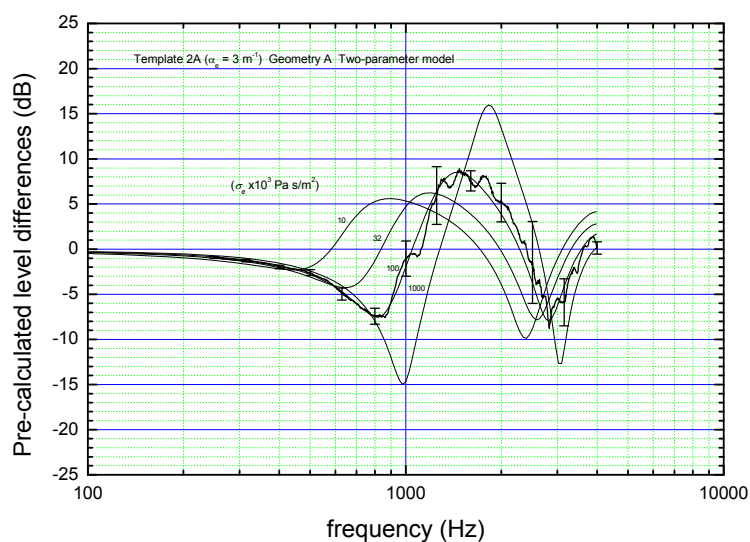


Figure A.8(a) – Template for geometry A and the two-parameter model with superimposed NRC data

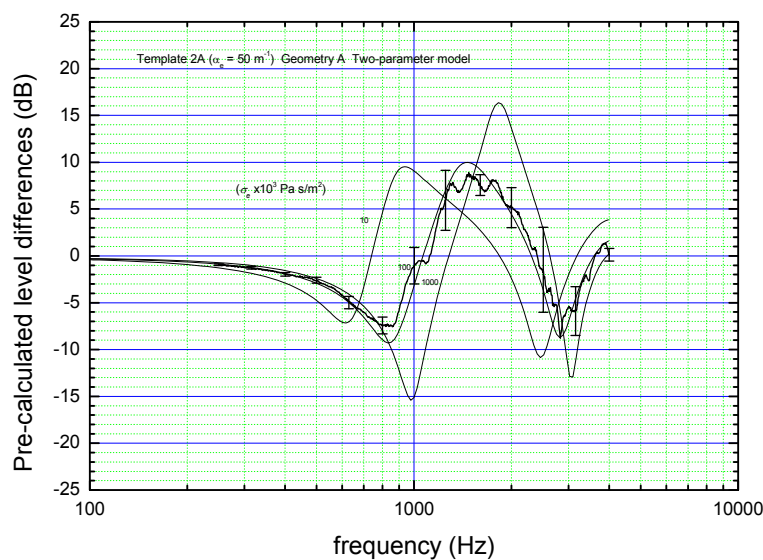


Figure A.8(b) – Template for geometry A and the two-parameter model with superimposed NRC data

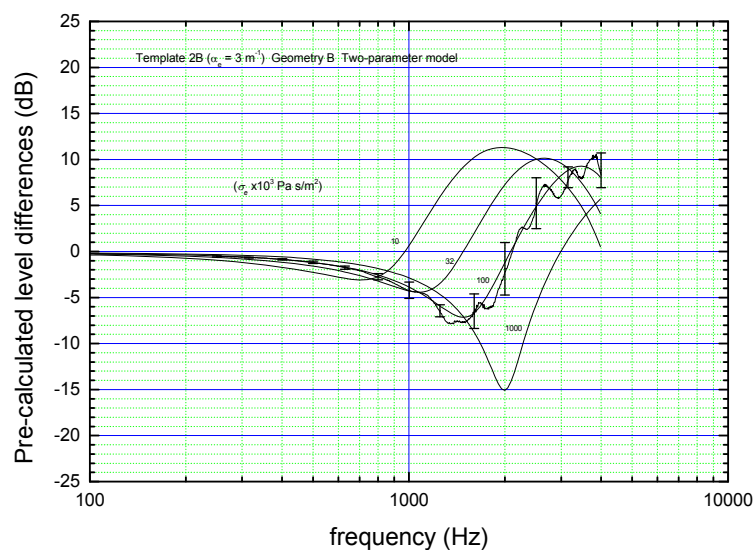


Figure A.9(a) – Template for geometry B and the two-parameter model with superimposed NRC data

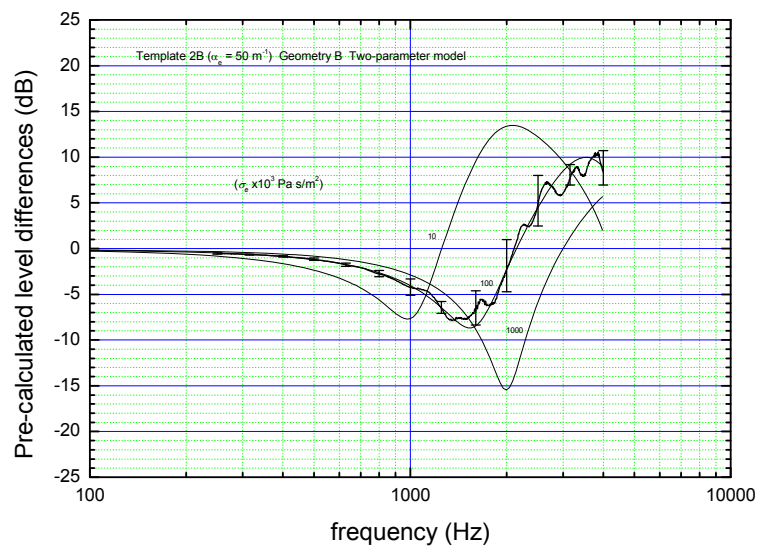


Figure A.9(b) – Template for geometry B and the two-parameter model with superimposed NRC data

Step 2 - Complex sound pressure ratio method

The measured complex sound pressure ratios were averaged, and the procedure outlined in 4.7 was used to determine the real and imaginary parts of the normalized specific acoustic impedance ratio at each measured frequency.

Step 3 - Smoothing

The result of Step 2 for geometry A is shown in Figure A.10. A 5-point moving average method was used to smooth the data. The smoothed data are shown in Figure A.6. The normalized specific acoustic impedance ratio data obtained in the case of geometry B are sufficiently smooth that Step 3 is not considered necessary. Hence this step is omitted for geometry B.

Step 4 - Comparisons

The real and imaginary parts of the normalized specific acoustic impedance ratio deduced from Steps 1 and 2 are shown in Figure A.11 and A.12 for geometry A and B, respectively. The solid lines represent the one-parameter model predictions. The dashed and dotted lines represent the predictions of the two-parameter model for $\alpha_e = 3$ and 50 m^{-1} , respectively.

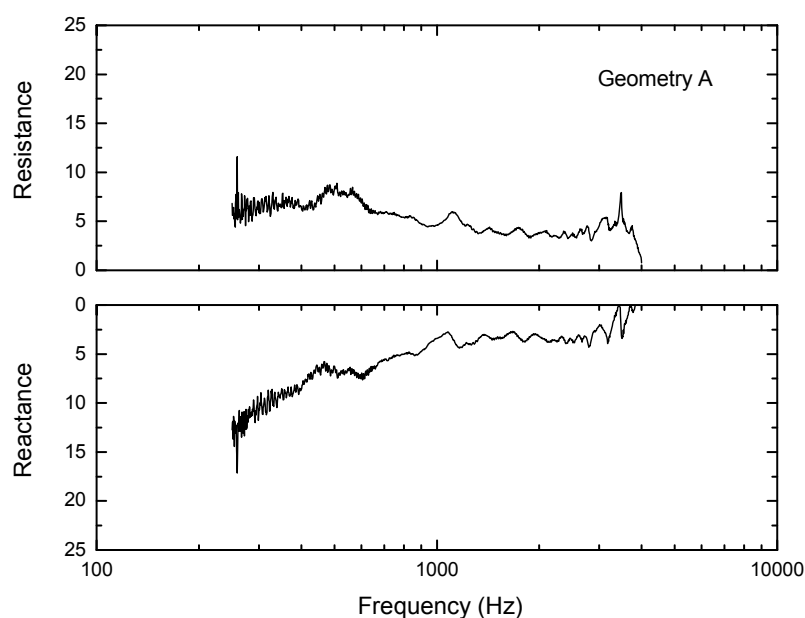


Figure A.10 – Normalized specific acoustic impedance ratio deduced from the measured complex sound pressure ratios using geometry A

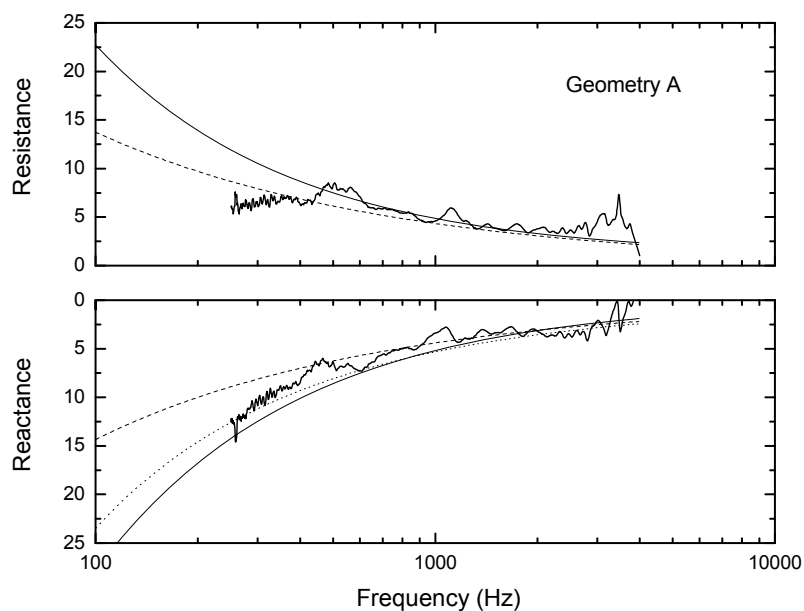


Figure A.11 – Normalized surface impedance spectra deduced from Step 1 (one-parameter model – solid line, two parameter model – dash and dotted line) and Step 2 (thicker continuous lines)

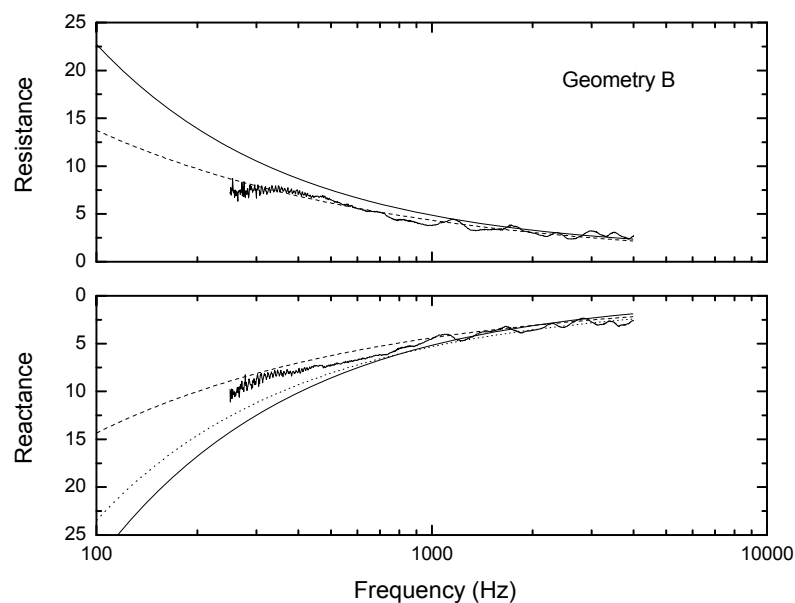


Figure A.12 – Normalized surface impedance spectra deduced from Step 1 (one-parameter model – solid line, two parameter model – dashed lines and dotted line) and Step 2 (thicker continuous lines)

A.3 Example 3: University lawn in Germany

Step 1

This example shows results obtained over a mown lawn where the measurement procedure did not include the switching of microphone positions. Moreover, the procedure used a version of geometry A that deviates significantly from that specified in this Standard (the lower microphone height was 0.05 m instead of 0.23 m). In these measurements an average of 10 measurements has been used. The LD spectral mean obtained from geometry A and B are plotted on each of the templates in Figures A.13 and A.14. The data represent values corresponding to the nearest one-third octave band center frequencies extracted from the narrowband data. The best least-squares fit is the one-parameter model with $\sigma_{eff} = 1000 \text{ kPa s/m}^2$ for geometry A and 320 kPa s/m^2 for geometry B.

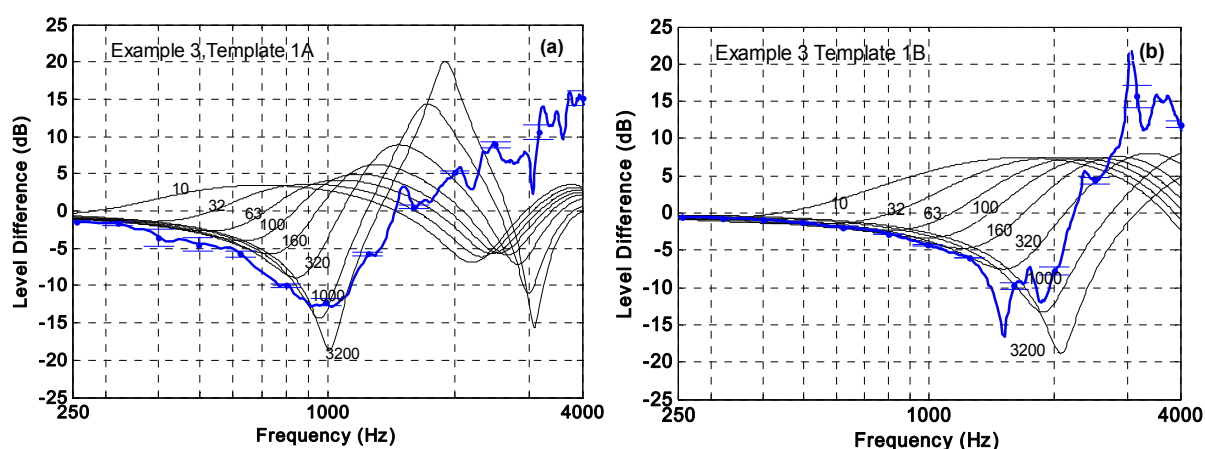


Figure A.13 – Data and one-parameter model templates for geometries A and B

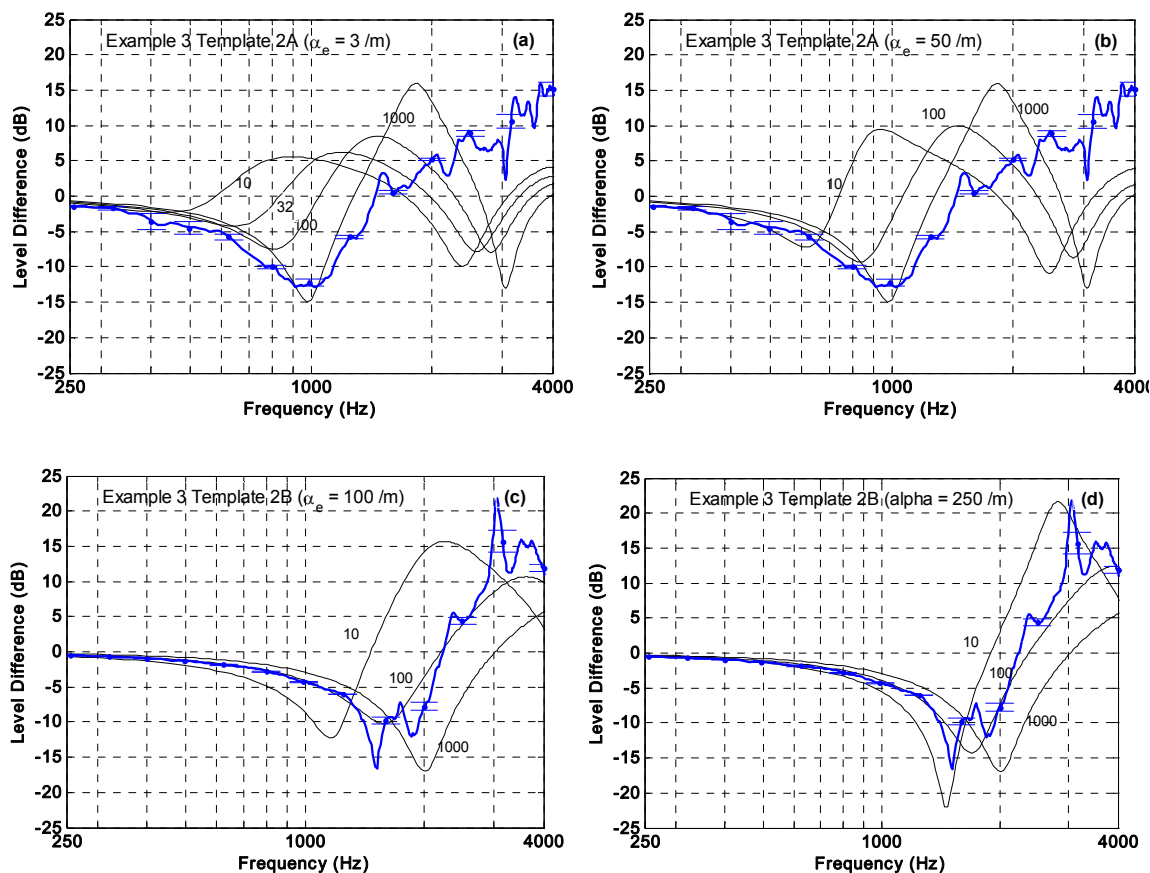


Figure A.14 – Data and 2-parameter model templates for geometries A and B

The cumulative errors, E , for both geometries are given in Table A.5.

Table A.5 – Cumulative error, E , for Example 2

Parameter, σ_{eff} (kPa s/m ²)	320	1,000
Geometry A	4200	4100
Geometry B	622	2300

Parameter: σ_e (kPa s/m ²); α_e (/m)	100; 3.0	100; 50	100; 100
Geometry A	4600	4800	5000
Geometry B	386	275	315

The deviations from the template curves above 1 kHz shown in Figures A.13 and A.14(a) and (b) are consistent with the fact that measurements have not used the recommended geometry A. It is clear that data using geometry B (which was correct) fits the templates better. Nevertheless, even when taking account of the geometry used in place of geometry A, the results (not shown) of the direct impedance deduction corresponding to geometry A are questionable. Hence, only the parameter values corresponding to best-fit geometry B results are taken forward to Step 2.

Step 2

Impedance spectra (see Figure A.8) have been deduced from the measured complex sound pressure ratios using geometry B. It is seen that impedance has small standard deviation (except possibly below 300 Hz). There is very little difference between mean of the ten deduced impedance spectra shown in Figure A.15 and the normalized surface impedance spectrum deduced from the mean of ten measured complex sound pressure ratios.

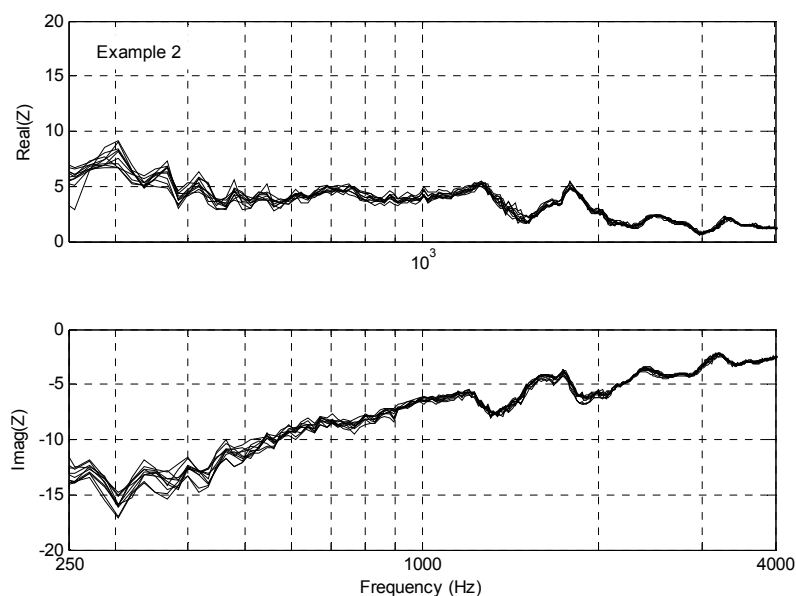


Figure A.15 – Deduced normalized surface impedance ratio spectra using all ten measurements

Step 3

Smoothing has been carried out using a 5-point moving average. Figure A.16 shows smoothed data as well as error bars at ± 1 Standard Deviation at one-third octave frequency points.

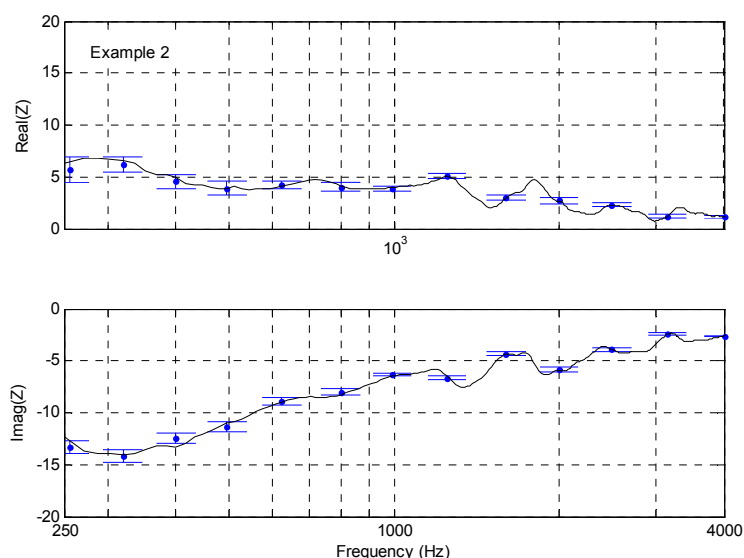


Figure A.16 – Smoothed normalized specific acoustic impedance ratio deduced using geometry B

Step 4

In Figure A.17 the ground impedance deduced by methods in Steps 1 and 2 are plotted together for geometry B. The solid lines are the smoothed deduced impedance spectra while asterisks indicate impedance spectrum from the best-fit one-parameter model from Table A.3, Step 1 and dots are those of the best-fit two-parameter model. Both models underestimate the imaginary part and overestimate the real part.

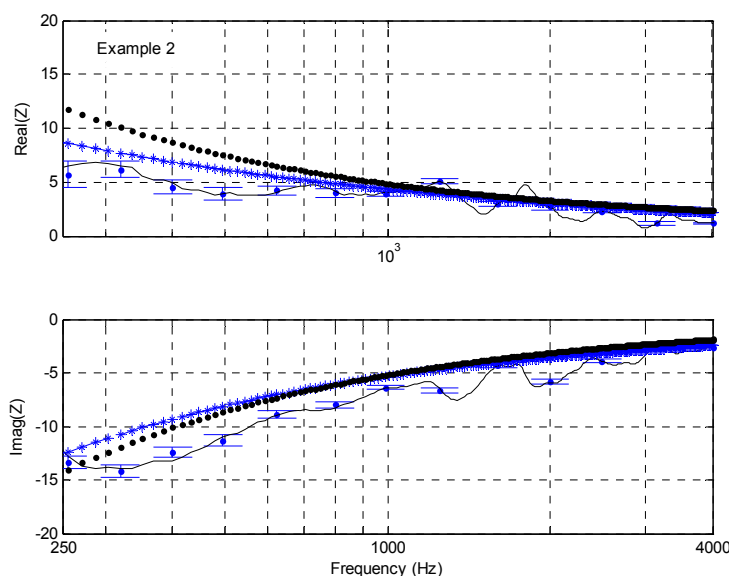


Figure A.17 – Normalized specific acoustic impedance ratio spectra deduced from both geometries A and B and best-fit impedance model predictions

A.4 Example 4: Granite gravel road on U.S. Army Research Laboratory testing facility

The source was a compression driver plus tube. Level difference (LD) spectra were recorded via a 16-bit A/D board using geometries A and B. Thirty seconds of data were recorded on each of four spots on the road with the selected source-microphone geometry. The microphones were switched and the measurements were repeated.

Temperature = 18°C, wind speed between 0.5 and 2.5 m/s (anemometer intermittent), the ground was compacted, contained many stones (~2 cm) and was saturated with water (there were pools of surface water in the vicinity of test area).

Step 1

The LD values (in dB) taken at each ground area were averaged and the standard deviations were computed. Average values, over all spots and two standard deviation error bars, were superimposed on Templates 1A and 1B [Figures A.18(a) and A.18(b)].

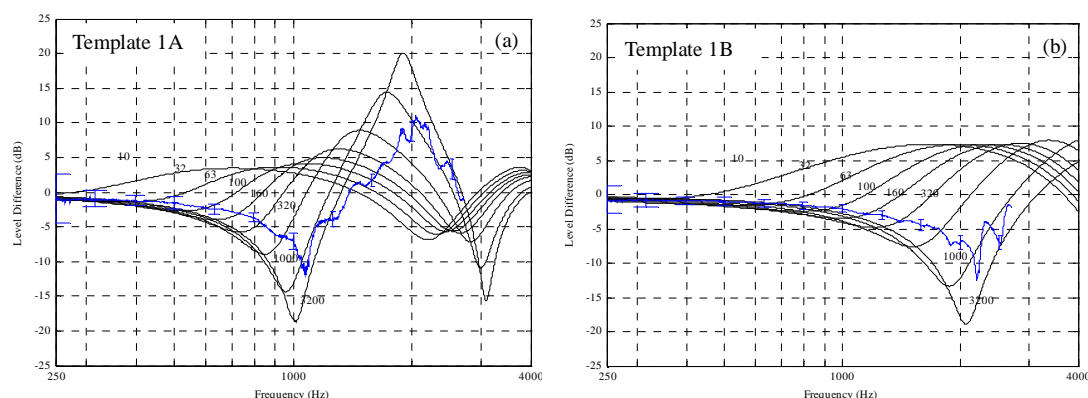


Figure A.18 – ARL data superimposed on one-parameter templates (a) geometry A and (b) geometry B

Data superimposed on templates for the two-parameter models are shown in Figure A.19(a) through A.19(h).

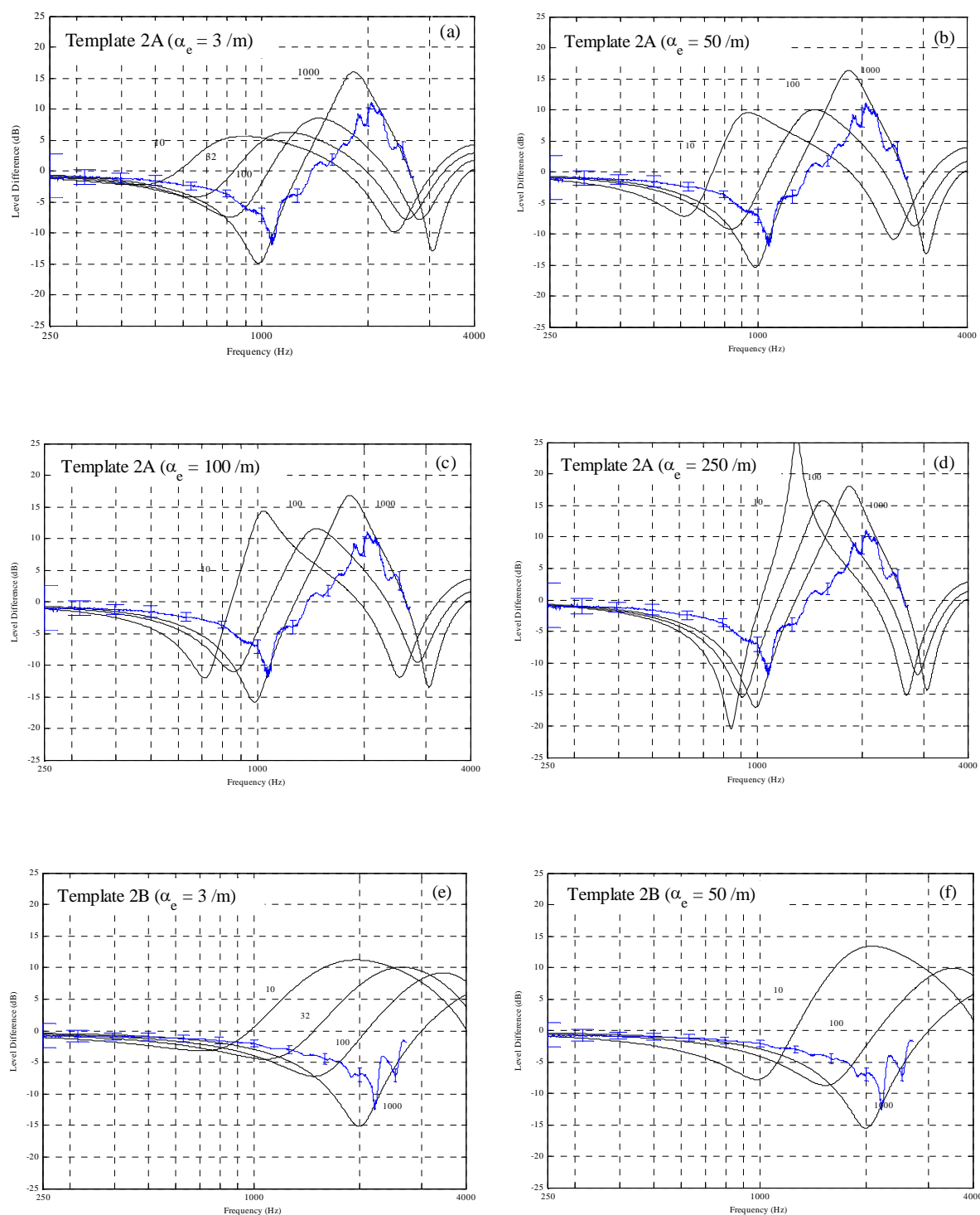


Figure A.19 (a) to (h) – ARL Gravel road data superimposed on two-parameter templates

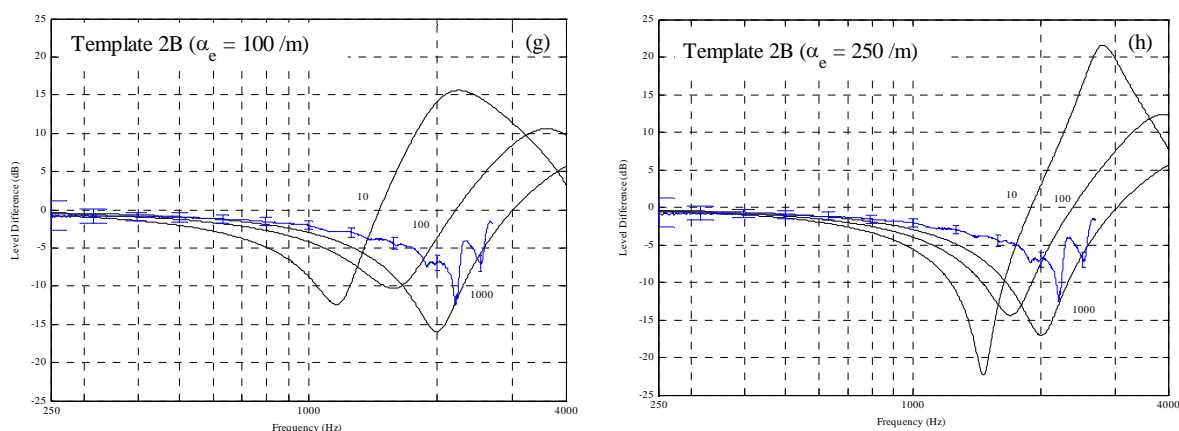


Figure A.19 a to h (continued) – ARL Gravel road data superimposed on two-parameter templates

None of the templates provide a particularly good fit. Indeed, cumulative errors, E , computed using Equation (8), 4.6 (not listed here), always yield values greater than 100,000. This is mainly the result of the ground being acoustically hard ($1000 \text{ kPa s/m}^2 < \sigma_e < 3200 \text{ kPa s/m}^2$ or $\sigma_{\text{eff}} > 1000 \text{ kPa s/m}^2$). Moreover, the presence of stones in the ground surface may have contributed to the higher frequency discrepancies as a result of scattering. As pointed out in Clause 4.5.1, the specified geometries are not appropriate for obtaining values for such high impedance and so it is not worth proceeding with Steps 2 through 4.

Annex B

(informative)

Example impedance parameters

B.1 One-parameter model

Table B.1 – Parameter values obtained using one-parameter model

Description of surface	Flow resistivity, σ_{eff} (kPa s/m ²)
Dry snow, newly fallen 0.1 m over about 0.4 m older snow	10-30
Sugar snow	25-50
In forest, pine, or hemlock	20-80
Grass: rough pasture, airport, public buildings, etc.	150-300
Roadside dirt, ill-defined small rocks up to 0.1 m mesh	300-800
Sandy silt, hard packed by vehicles	800-2500
Asphalt, sealed by dust and light use	30 000
Upper limit set by thermal-conduction and viscous boundary layer	2×10^5 to 1×10^6

B.2 Two-parameter model

Table B.2 – Parameter values obtained using two-parameter model

Description of surface	σ_e (kPa s/m ²)	α_e (/m)
Meadow with grass 8-10 cm high	227	121
Hay-covered field	188	50
Lawn	182	40
Institutional grass	100	3 - 50
Grass-covered field	100	250
Cricket field	70	25
Floor of pine forest	7.5	16
Thick newly fallen snow	5	0

Annex C

(informative)

Formulae for the complex sound pressure ratio

The complex pressure ratio at each and every frequency between two spatially separated microphones is written as the ratio of pressures at upper and lower microphones.

$$T(f) = \frac{p_u(f)}{p_l(f)} \quad (\text{C.1})$$

where

$$p(f) = \frac{1}{R_d} \exp[ikR_d] + Q(f, \beta) \frac{1}{R_r} \exp[ikR_r] \quad (\text{C.2})$$

In the above and the following expressions, subscripts u and l denote upper and lower microphones, respectively. R_d is the distance from the source to the receiver (direct path), R_r is the distance from the image source to the receiver (reflected path), and k is the wave number given by $k = 2\pi/\lambda$. The term β denotes the surface admittance and is a function of frequency. When using (C.2) to predict the sound field for a given geometry, β is calculated from an impedance model (such as those specified in 4.5.2 and 4.5.3 or user-defined).

The magnitude of the complex sound pressure ratio spectrum in dB (used in 4.5.1, Step 1), referred to elsewhere in this Standard as the level difference spectrum, is defined as:

$$LD(f) = 20 \log(|T(f)|) \quad (\text{C.3})$$

The direct and reflected paths are evaluated for upper and lower microphones from the following expressions:

$$R_d = \left[(h_s - h_r)^2 + R^2 \right]^{1/2} \quad (\text{C.4})$$

and

$$R_r = \left[(h_s + h_r)^2 + R^2 \right]^{1/2} \quad (\text{C.5})$$

Given that

$$W(w) = e^{-w^2} \operatorname{erfc}(-iw) \quad (\text{C.6})$$

and

$$\tau = \sqrt{\frac{1}{2} ikR_r} \quad (\text{C.7})$$

The angle of incidence is θ and the numerical distance, w , is given by:

$$w = \tau(\cos \theta + \beta) \quad (\text{C.8})$$

The reflection coefficient, Q , and its derivative with respect to the specific surface admittance, β , are given by:

$$Q = 1 + 2\tau\beta \left[i\sqrt{\pi}W(w) \right] \quad (\text{C.9})$$

$$Q' = \frac{dQ}{d\beta} = 2\tau \left[i\sqrt{\pi}W(w) - 2\tau\beta \left(1 + i\sqrt{\pi}wW(w) \right) \right] \quad (\text{C.10})$$

The derivative, with respect to admittance, of the Complex pressure ratio required in Newton-Raphson method (which is used in the minimization method described in 5.7) is given by

$$T'(\beta) = \frac{dT}{d\beta} = T(\beta) \left[\frac{Q'_u(\beta) \exp(ikR_{u,r})}{L_u(\beta)R_{u,r}} - \frac{Q'_l(\beta) \exp(ikR_{l,r})}{L_l(\beta)R_{l,r}} \right] \quad (\text{C.11})$$

where L_u and L_l are defined in (C.2).

A procedure for computing the special function, $W(z)$, is given in Annex D.

Annex D

(informative)

Mathematical functions

The series representation of $W(z)$ for a complex argument z is given by:

$$W(z) = e^{-z^2} \operatorname{erfc}(-iz) = \sum_{n=0}^{\infty} \frac{(iz)^n}{\Gamma(\frac{n}{2} + 1)} \quad (\text{D.1})$$

where $\Gamma(x)$ is the Gamma function.

For large z the following asymptotic expansion may be used:

$$\sqrt{\pi} z \exp(z^2) \operatorname{erfc}(z) \sim 1 + \sum_{m=1}^{\infty} (-1)^m \frac{1.3 \dots (2m-1)}{(2z^2)^m} \text{ for } \left(z \rightarrow \infty, |\arg z| < \frac{3\pi}{4} \right) \quad (\text{D.2})$$

(Note that this expression can be written in terms of $W(z)$ function also but is given in this form in the reference. Simply replace z by $-iz$.)

The numerical computation of the error function can be implemented easily by using the following formulae for a large range of $|z|$. Note that the numerical distance is expressed in its real and imaginary parts as, $z = z_r + iz_x$.

According to Abramowitz and Stegun [Ref. 5, p. 328], if $z_r > 3.9$ or $z_x > 3$,

$$W(z) = iz \left(\frac{0.461315}{z^2 - 0.1901635} + \frac{0.09999216}{z^2 - 1.7844927} + \frac{0.002883894}{z^2 - 5.5253437} \right) \quad (\text{D.3})$$

with an absolute error of less than 2×10^{-6} . If $z_r > 6$ or $z_x > 6$,

$$W(z) = iz \left(\frac{0.5124242}{z^2 - 0.2752551} + \frac{0.05176536}{z^2 - 2.724745} \right) \quad (\text{D.4})$$

with an absolute error less than 1×10^{-6} .

For smaller values of z_r and z_x , the Matta and Reichel formula [6] may be used:

$$W(z) = [W_r(z_r, z_x) - z_x E(\Delta)/\pi] + i[W_x(z_r, z_x) + z_r E(\Delta)/\pi] \quad (D.5)$$

where $E(\Delta)$ is an error term with its bound given by:

$$E(\Delta) \leq \frac{2\sqrt{\pi}e^{-\pi^2/\Delta^2}}{1 - e^{-\pi^2/\Delta^2}}, \quad (D.6)$$

The value of the error bounds variable, Δ (≤ 1), is set according to the required accuracy (see discussion after (D.10)).

$$W_r(z_r, z_x) = \frac{z_x \Delta}{\pi(z_r^2 + z_x^2)} + \frac{2z_x \Delta}{\pi} \sum_{n=1}^{\infty} \frac{e^{-n^2 \Delta^2} (z_x^2 + z_r^2 + n^2 \Delta^2)}{(z_x^2 - z_r^2 + n^2 \Delta^2)^2 + 4z_x^2 z_r^2} \quad (D.7)$$

$$\begin{aligned} &+P \quad \text{if} \quad z_x < \pi/\Delta, \\ &+\frac{1}{2}P \quad \text{if} \quad z_x = \pi/\Delta, \\ &+0 \quad \text{if} \quad z_x > \pi/\Delta, \end{aligned}$$

$$W_x(z_r, z_x) = \frac{z_r \Delta}{\pi(z_r^2 + z_x^2)} + \frac{2z_r \Delta}{\pi} \sum_{n=1}^{\infty} \frac{e^{-n^2 \Delta^2} (z_x^2 + z_r^2 - n^2 \Delta^2)}{(z_x^2 - z_r^2 + n^2 \Delta^2)^2 + 4z_r^2 z_x^2} \quad (D.8)$$

$$\begin{aligned} &-Q \quad \text{if} \quad z_x < \pi/\Delta, \\ &-\frac{1}{2}Q \quad \text{if} \quad z_x = \pi/\Delta, \\ &+0 \quad \text{if} \quad z_x > \pi/\Delta, \end{aligned}$$

$$\begin{cases} P = 2e^{-[z_r^2 + (2z_x \pi/\Delta) - z_x^2]} \left[\frac{A_1 C_1 - B_1 D_1}{C_1^2 + D_1^2} \right] \\ Q = 2e^{-[z_r^2 + (2z_x \pi/\Delta) - z_x^2]} \left[\frac{A_1 D_1 + B_1 C_1}{C_1^2 + D_1^2} \right] \end{cases} \quad (D.9)$$

with

$$\begin{cases} A_1 = \cos(2z_r z_x) \\ B_1 = \sin(2z_r z_x) \\ C_1 = e^{-2z_x \pi/\Delta} - \cos(2z_r \pi/\Delta) \\ D_1 = \sin(2z_r \pi/\Delta) \end{cases} \quad (D.10)$$

If $\Delta = 1$, then $|E(\Delta)| \leq 10^{-4}$. Only three or four terms are needed for the infinite sums in $W_r(z_r, z_x)$ and $W_x(z_r, z_x)$ in order to meet this requirement. If $\Delta = 0.8$, then the magnitude of the error term

becomes less than 10^{-6} . In this case, summing the series up to the fifth term will be sufficient to guarantee the required accuracy.

The formula given above is valid only for $z_r > 0$ and $z_x > 0$. However, in practice, only the first quadrant in the complex z plane need be computed. The rest of the values can be evaluated by noting the following symmetry relations of Error functions:

$$W(-z) = 2\exp(-z^2) - W(z) \quad (\text{D.11})$$

$$W(\bar{z}) = \overline{W(z)} \quad (\text{D.12})$$

Annex E

(informative)

Software for deduction of surface impedance according to ANSI/ASA S1.18-2010

The procedure for calculating normalized surface impedance from level difference measurements used here is essentially the same as described in [2]. Executable and compilable versions of Fortran code for calculating impedance according to this procedure are provided with this Standard. Also provided is MatLab[®] script version of the procedure together with example input and output files. This is a slightly modified form of a script developed originally at the National Research Council of Canada. The files used to specify the format of input and output for running each code together with example level difference spectra input and impedance spectra output are provided.

The software provided with this American National Standard is entirely informative and provided only for the convenience of the user. Use of the provided software is not required for conformance with the Standard. The software is not warranted to be appropriate for any particular purpose. No warranties or guarantees are provided.

Bibliography

- [1] H.M. Hess, K. Attenborough, and N.W. Heap. "Ground characterization by short-range propagation measurements", *J. Acoust. Soc. Am.* 87(5), 1975-1986 (1990).
- [2] S. Taherzadeh and K. Attenborough. "Deduction of ground impedance from measurements of excess attenuation spectra", *J. Acoust. Soc. Am.* 105(3), 2039-2042 (1999).
- [3] C. Nocke, T. Waters-Fuller, K. Attenborough, V. Mellert, and K.M. Li. "Impedance deduction from broad-band, point-source measurements at grazing angles", *Acustica Combined with Acta Acustica*, **83**, 1085-1090 (1997).
- [4] R. Kruse and V. Mellert. "Effect and minimization of errors in in-situ ground impedance measurements", *Applied Acoustics* **69**, 884-890 (2008).
- [5] M. Abramowitz and I.A. Stegun. *Handbook of Mathematical Functions*, Chapter 7, Dover Publ., New York.
- [6] F. Matta and A. Reichel. "Uniform computation of the error function and other related functions," *Mathematics of Computation*, **25**, 339-344 (1971).
- [7] ANSI/ASA S12.18, *American National Standard Procedures for Outdoor Measurement of Sound Pressure Level*.
- [8] ANSI/ASA S12.8, *American National Standard Methods for Determining Insertion Loss of Outdoor Noise Barriers*.
- [9] ANSI S1.26, *American National Standard Method for the Calculation of the Absorption of Sound by the Atmosphere*.
- [10] ISO 9613-1:1993 *Acoustics – Attenuation of sound during propagation outdoors – Part 1: Calculation of the absorption of sound by the atmosphere*.

MEMBERS OF THE ASA COMMITTEE ON STANDARDS (ASACOS)

P.D. Schomer, *Chair and ASA Standards Director*

Schomer and Associates
2117 Robert Drive
Champaign, IL 61821
Tel: +1 217 359 6602
Fax: +1 217 359 3303

R.D. Hellweg, Jr., *Vice Chair*

Hellweg Acoustics
13 Pine Tree Road
Wellesley, MA 02482
Tel: +1 781 431 9176

S.B. Blaeser, *Standards Manager*

Standards Secretariat
Acoustical Society of America
35 Pinelawn Rd., Suite 114E
Melville, NY 11747
Tel: +1 631 390 0215
Fax: +1 631 390 0217
Email: asastds@aip.org

Representation S1, Acoustics

P. Battenberg, *Chair, S1*
R.J. Peppin, *Vice Chair, S1*
A.H. Marsh, *ASA Representative, S1*
P.D. Schomer, *ASA Alternate Representative, S1*

Representation S2, Mechanical Vibration and Shock

A.T. Herfat, *Chair, S2*
C.F. Gaumond, *Vice Chair, S2*
ASA Representative, S2
B.E. Douglas, *ASA Alternate Representative, S2*

Representation S3, Bioacoustics

C.A. Champlin, *Chair, S3*
ASA Representative, S3
G.J. Frye, *Vice Chair, S3*
M.D. Burkhard, *ASA Alternate Representative, S3*

Representation S3/SC1, Animal Bioacoustics

D.K. Delaney, *Chair, S3/SC1*
M.C. Hastings, *Vice Chair, S3/SC1*
ASA Representative, S3

Representation S12, Noise

W.J. Murphy, *Chair, S12*
R.D. Hellweg, *Vice Chair, S12*
ASA Representative, S12
D. Lubman, *ASA Alternate Representative, S12*

ASA Technical Committee Representation

A.P. Lyons, *Acoustical Oceanography*
A.E. Bowles, *Animal Bioacoustics*
A. Campanella, *Architectural Acoustics*
P.J. Kaczkowski and V. Khokhlova, *Biomedical Ultrasound/Bioresponse to Vibration*
R.M. Drake, *Engineering Acoustics*
D. Deutsch, *Musical Acoustics*
R.J. Peppin, *Noise*
R. Raspet, *Physical Acoustics*
J. DiGiovanni, *Psychological and Physiological Acoustics*
C.F. Gaumond, *Signal Processing in Acoustics*
S. Narayanan, *Speech Communication*
D. Capone, *Structural Acoustics and Vibration*
R.M. Drake, *Underwater Acoustics*

Ex Officio Members of ASACOS

J.R. Dubno, *Chair, ASA Technical Council*
D. Feit, *ASA Treasurer*
T.F.W. Embleton, *Past Chair ASACOS*
C.E. Schmid, *ASA Executive Director*

U. S. Technical Advisory Group (TAG) Chairs for International Technical Committees

P.D. Schomer, *Chair, U. S. TAG, ISO/TC 43*
V. Nedzelnitsky, *Chair, U. S. TAG, IEC/TC 29*
D.J. Evans, *Chair, U. S. TAG, ISO/TC 108*



ANSI/ASA S1.18-2010
(revision of ANSI S1.18-1999)